

ION INJECTION INTO
RADIO FREQUENCY
QUADRUPOLE FIELD DEVICES

by

Sidney Luther Gulick

A thesis submitted to the
Faculty of Graduate Studies and Research
in partial fulfillment of the requirements
for the degree of Master of Science

Foster Radiation Laboratory
McGill University, Montréal
Québec, Canada

© January, 1986

ABSTRACT

The mathematical basis for the operation of radio-frequency quadrupole devices is described and related to the operation of real devices. The design, construction and operation of an rfq mass filter and ion trap are documented. Experiments are described which provide an estimate of the absolute number of ions in a trap and the efficiency with which a trap can confine and retain ions produced outside the trap and injected into it:

RÉSUMÉ

Les bases mathématiques pour l'opération d'appareils à champ quadrupolaire électrique de radiofréquence sont décrites et reliées à des appareils réels. La conception, la construction et l'opération d'un filtre de masse et d'un piège à ions à base de champ quadrupolaire électrique de radiofréquence sont documentées. Des expériences sont décrites qui donnent une estime du nombre absolu d'ions dans le piège et de l'efficacité avec laquelle un piège peut confiner et retenir des ions produits à l'extérieur et qui lui sont injectés.

ACKNOWLEDGEMENTS

I would like to thank the following people and institutions for making my work at McGill possible and (most of the time) enjoyable:

My wife Hannelore and my daughter Irmgard Frances, for their emotional support and understanding through what were difficult times for us all;

My advisor Prof. R. Moore and my colleague G. Rouleau, who shared my trials and aided me in my work;

My colleague D. Lunney, who did most of the groundwork on the trap project;

Steve Kecani, Leo Nikinnen, Mario Della Neve and Carl Jorgensen, who along with Moore, Rouleau and Lunney helped design and build my apparatus and get it going;

The Foster Radiation Laboratory, NSERC, and the McGill Physics Department, who provided the equipment and financial support I needed to carry out my studies and research;

My friend D. Young, for help with my drawings;

Guy Savard, for turning my abstract into a resume;

Michael Bodnar, for help with circuitry and general good spirits during the summer of 1985;

A. Al-Alousi, for a thorough proof-reading;

Prof. J. Crawford, for assistance with both research and academic work;

My parents, who gave me help when I needed it and left me

alone when I needed that;

My grandfather, for general inspiration;

and finally my dog George, who did what a dog does best
and did it as well as he was able--who could ask more of
anyone?

TABLE OF CONTENTS

ABSTRACT

RÉSUMÉ

ACKNOWLEDGEMENTS

LIST OF FIGURES

I INTRODUCTION 1

STATEMENT OF PURPOSE

HISTORICAL PERSPECTIVE

REFERENCES--I

II MATHEMATICAL BASIS OF QUADRUPOLE FIELD DEVICES 7

THE QUADRUPOLE FIELD GEOMETRY

EQUATIONS OF MOTION--IDEAL DEVICES

ANALYTICAL SOLUTIONS TO THE HILL AND MATHIEU EQUATIONS

MATHIEU STABILITY DIAGRAM

REFERENCES--II

III REAL DEVICES 24

NUMERICAL METHODS--A BRIEF SURVEY

SIMPLE MODELS OF ION TRAPS AND THE EFFECTS
OF SPACE CHARGE

FISCHER'S MODEL

DEHMELT'S MODEL

AN EMPIRICAL APPROACH

CAPTURE--LOSS RATE LAW

REFERENCES--III

IV EXPERIMENTAL PROCEDURE AND RESULTS

43

APPARATUS

VACUUM SYSTEM

ION GUN

MASS FILTER

EXPERIMENTAL RESULTS

ION TRAP

RESONANT DETECTION SYSTEM

DATA ACQUISITION SYSTEM

TRAP EXPERIMENTAL DATA AND RESULTS

REFERENCES--IV

V CONCLUSIONS

77

LIST OF FIGURES

Figure 1.	Quadrupole field equipotential lines	18
2.	a. Mass filter ideal electrode structure b. Ion trap ideal electrode structure	
Figure 3.	Mathieu function stability diagram	19
Figure 4.	a. Mass filter stability diagram b. Detail showing first region of stability	20
Figure 5.	a. Ion trap stability diagram b. Detail showing first region of stability	21
Figure 6.	Photographs of microparticles in a trap	40
Figure 7.	Vacuum system--block diagram	62
Figure 8.	Ion gun with mounting plate	63
Figure 9.	Mass filter details	64
Figure 10.	Mass filter system--block diagram	65
Figure 11.	Mass filter rectifier and DC supply	66
Figure 12.	Trap assembly details	67
Figure 13.	Ion gun - ion trap assembly	68
Figure 14.	Trap detail showing hole in end cap	69
Figure 15.	Ion trap demodulator-amplifier circuit	70
Figure 16.	Ion trap system--block diagram	71
Figure 17.	Representative traces taken with no buffer gas (10^{-7} torr)	72
Figure 18.	Traces showing effects of buffer gas on peak shape and amplitude	73
Figure 19.	Successive traces showing frequency shift, fill rate and peak broadening (10^{-4} torr)	74

References for each chapter are listed at the end of the chapter; a complete bibliography follows the last chapter.

I INTRODUCTION

STATEMENT OF PURPOSE

There are two main purposes to this thesis: first, to document the establishment of an experimental facility to study the characteristics and possible applications of radio-frequency quadrupole field mass selective devices; and second, to describe initial results of investigation into the possibility of injecting ions into a rfq trap and retaining them for a significant period of time. Over the past two years the author, with the help of students, faculty and staff of the Foster Radiation Laboratory of McGill University's Physics Department, has assembled a vacuum system capable of pressures on the order of 5×10^{-8} Torr; constructed a tractable ion source with an output of up to 100 nanoamperes with energy variable from 0-200eV and pulsable with pulse widths down to 3 microseconds; designed, assembled and tested an rfq mass filter and a suitable power supply enabling the filter to be operated both in a low-resolution, high-transmission mode and a medium-resolution (around 50) mode tunable over a mass range of 0-150 u; assembled and tested an rfq ion trap with power supply and detection circuitry; and assembled and tested a microprocessor-controlled digital data acquisition system with 8-bit resolution enabling acquisition, storage, and

rapid display of the output of the ion trap detection circuitry. These systems were used to inject ions produced in an external controllable ion gun so as to investigate possible capture mechanisms. To the author's knowledge this is the first time controlled ion injection into a trap has been performed.¹ Experiments have been performed which provide an estimate by new means of the number of ions in an rfq trap² and a measurement has been made of the efficiency with which the trap captures externally produced ions injected along the z-axis.

HISTORICAL PERSPECTIVE

Historically the first rfq filters and traps were constructed by Wolfgang Paul and his colleagues at the University of Bonn during the period 1953-1955³. The principles governing the operation of the devices were suggested by the work of Courant, Livingston and Snyder developing the concepts of strong focusing of proton beams through alternating gradient magnetic quadrupole fields in their work at Brookhaven National Laboratory⁴. The differential equations describing the motions of ions in the fields associated with rfq mass-selective devices had been investigated much earlier; Mathieu had in 1868 introduced the functions bearing his name in mathematical literature to describe the modes of oscillation of an elliptically bounded diaphragm, while Hill dealt with the more general equation of which the Mathieu equation is a special case in his study of

the 'mean motion of the lunar perigee' in 1877₅. Analytical treatment of real devices remains extremely difficult especially when device tolerances and fringing fields are taken into account. However the rapid development of digital computers over the past 30 years has resulted in deeper understanding of the functioning of rfq devices through application of numerical calculation of fields and trajectories. Application of matrix and phase-space beam optics offers further insights into the operation of actual devices.

Rfq mass filters and traps both possess certain characteristics which give them distinct advantages over the magnetic spectrometers which were in common use when the rfq devices first appeared. For the mass filter these include ease of construction, absence of magnetic fields, easy adjustment of and tradeoff between sensitivity and resolution, light weight due to absence of iron cores for magnets, linear mass scale, and the possibility of high-speed electronic scanning. The trap potentially offers these advantages and in addition the ability to integrate the ion formation rate. Furthermore the 3-dimensional trajectory avoids the limitations to resolution posed by length in the mass filter. These advantages coupled with a large increase in the routine application of high and ultra-high vacuum technology have resulted in a rapid development of quadrupole spectrometry which contrasts markedly with the slow evolution

- 4 -

of the magnetic devices.

Presently the mass filter is fairly well understood; current developments are mainly in the field of applications and large numbers of commercial products using rfq filters are available on the market today. The rfq trap is a less fully explored topic. Its theoretical potential as a high-resolution, compact, sensitive spectrometer has not been fully realized to this date and its potential as a means of storing ions produced at a slow rate is hampered by the fact that one must get the ions into the trap efficiently in order to benefit from the ability to retain them there.₆

REFERENCES--I

1. Schuessler, H.; O, C.; "Trapping of Ions Injected From An External Source Into A Three-Dimensional Quadrupole Trap", Nuclear Instruments and Methods 186 (1981), 219-30. Describes numerical simulation of ion injection; no experiments reported.
2. Schuessler, H.; Fortson, E.; Dehmelt, H.; "Hyperfine Structure of the Ion-Storage Exchange-Collision Technique", Physical Review V.187, #1, 5 November 1969, pp. 23-26 gives an exhaustive description of a similar calculation but a critical assumption is that the ions are driven against the electrodes and lost; the present experiments show that with a buffer gas as a damping mechanism the ion loss rate seems independent of the detection drive.
3. Paul, W.; Steinweidel, H.; Z. Naturforsch A., 8 (1953) p.448
4. Courant, Livingston, Snyder, Physical Review 88 (1952), p, 1190
5. McLachlan, N. W.; Theory and Application of Mathieu Functions, Oxford at the Clarendon Press, 1947. Chapter 1 gives a good description of the mathematical history of work on these types of function.
6. Quadrupole Mass Spectrometry and its applications, Peter H. Dawson, editor; Elsevier Scientific Publishing company, New York, 1976. This is the most complete reference found by

~~the~~ author; extensive use was made throughout the present work of this lucid and complete compendium of the history and techniques of the art. Chapter 1 contains a concise history and a survey of the many applications of the rf quadrupole field.

II MATHEMATICAL BASIS OF QUADRUPOLE FIELD DEVICES

THE QUADRUPOLE FIELD₁

The fundamental characteristic of the quadrupole field is the linear dependence of the field vector \underline{E} on coordinate position. In cartesian coordinates

$$\underline{E} = E_0(jx\mathbf{l}_x + ky\mathbf{l}_y + lz\mathbf{l}_z)$$

where j , k , l are weighting constants; \mathbf{l}_x , \mathbf{l}_y , \mathbf{l}_z are unit vectors in the x , y , and z directions; and E_0 is a term common to the 3 components of \underline{E} . The fact that this equation is decoupled in three directions makes it possible to consider motion in each direction separately. This model is absolutely valid only in perfect devices. The approximation is close enough to give a fairly accurate picture of the fundamental nature of the ion motion in real devices although its value in terms of numerical prediction of actual results is limited.

In order to satisfy Maxwell's Divergence equation, if there is no charge inside the electrode structure of a particular device,

$$\text{div. } \underline{E} = 0, \text{ so that}$$

$$j + k + l = 0.$$

Two simple sets of values which satisfy this condition are

$$a) \quad j = -k, \quad l = 0;$$

$$b) \quad j = k, \quad l = -2j$$

with case a) applying to the mass filter and case b) applying

to the three-dimensional rfq ion trap.

A potential distribution giving rise to a field of this type is

$$P = (-E_0/2)(jx^2 + ky^2 + lz^2).$$

(See figure 1 for a diagram of a two-dimensional potential distribution giving rise to a quadrupole field.)

EQUATIONS OF MOTION--IDEAL DEVICES

The ideal mass filter consists of four hyperbolic cylinders, infinitely long, arranged with a four-fold symmetry about the z-axis (see figure 2a). If the distance between opposite cylinders is $2r_0$ and the potential between adjacent electrodes is P_0 then

$$P = (P_0/2r_0^2)(x^2 - y^2) \text{ with}$$

$$E_0 = -P_0/r_0^2.$$

The ideal ion trap is a three-electrode structure with two end-caps and a ring electrode. A cross-section in the r-z plane shows complementary hyperbolae with a ratio of $2^{1/2}$ of the semiaxes (r_0/z_0) (see figure 2b). If P_0 is applied between the ring and the end caps then inside the trap

$$P = (P_0/2r_0^2)(r^2 - 2z^2).$$

For the mass filter the equations of motion are thus

$$d^2x/dt^2 + P_0ex/mr_0^2 = 0$$

$$d^2y/dt^2 - P_0ey/mr_0^2 = 0$$

$$d^2z/dt^2 = 0$$

with ions of charge e and mass m , neglecting gravitational

forces.

For the ion trap,

$$d^2x/dt^2 + P_0ex/mr_0^2 = 0$$

$$d^2y/dt^2 + P_0ey/mr_0^2 = 0$$

$$d^2z/dt^2 - 2P_0ez/mr_0^2 = 0.$$

In cylindrical coordinates, with $x=r\cos\phi$ and $y=r\sin\phi$, the first two equations for the ion trap may be transformed into the equivalent equations

$$d^2r/dt^2 - r(d\phi/dt)^2 + P_0er/mr_0^2 = 0$$

$$2(dr/dt)(d\phi/dt) + r(d^2\phi/dt^2) = 0.$$

The latter equation yields the result that $r^2d\phi/dt$ is a constant; angular momentum is conserved in the trap. The former equation may thus be written in the form

$$d^2r/dt^2 + P_0er/mr_0^2 = L^2/r^3 \text{ with}$$

$$L = r^2d\phi/dt.$$

The term containing L may be thought of as similar to a centripetal force and makes it impossible for an ion with an initial angular velocity to reach the center of the trap. For most applications the angular velocity may be considered as negligible in which case the equation in r for the ion trap becomes

$$d^2r/dt^2 + P_0er/mr_0^2 = 0.$$

In sinusoidally driven devices the potential P_0 is chosen to be of the form $(U - V\cos\omega t)$ with U being half the DC and V being half the peak AC voltages applied between adjacent electrodes, and ω being the angular frequency of the rf drive

($\omega = 2\pi \times$ the rf frequency). Make the following substitutions:

for the mass filter

$$a_u = a_x = -a_y = 4eU/m\omega^2 r_o^2$$

$$q_u = q_x = -q_y = 2eV/m\omega^2 r_o^2$$

$$Z = \omega t/2$$

while for the ion trap

$$a_u = a_z = -2a_r = -4eU/m\omega^2 r_o^2$$

$$q_u = q_z = -2q_r = -2eV/m\omega^2 r_o^2.$$

Making the substitutions in the relevant equations of motion puts each of the equations in the form

$$d^2u/dZ^2 + (a_u - 2q_u \cos 2Z)u = 0$$

which is the canonical form of the Mathieu equation.

ANALYTICAL SOLUTIONS TO THE HILL AND MATHIEU EQUATIONS

As mentioned before the equations of motion of particles in rfq devices may be reduced to equations of the form

$$(1) \quad d^2U/dZ^2 + (A_0 + \sum_s (2A_s \cos 2sZ)) \times U = 0$$

where the \sum indicates summation over s from 1 to infinity and the summed term represents any function W of period π . Floquet's theorem states that for any second-order differential equation with periodic coefficients there exists a solution U such that

$$U(Z + 2\pi) = K \times U(Z)$$

where K is a complex constant.

Let

$$K = e^{\mu\pi};$$

Construct

$$P(Z) = e^{-\mu Z} U(Z); \text{ then}$$

$$\begin{aligned} P(Z + \pi) &= e^{-\mu\pi} e^{-\mu Z} U(Z + \pi) \\ &= e^{-\mu Z} e^{-\mu\pi} K U(Z) \\ &= e^{-\mu Z} U(Z) \\ &= P(Z) \end{aligned}$$

so that P is periodic with period π and may thus be represented by the series

$$\sum_n C_{2n} e^{2inZ},$$

n including negative and positive integers, and U may be written in the form

$$(2) \quad e^{\mu Z} \sum_n C_{2n} e^{2inZ}.$$

Write

$$\underline{S}_s 2A_s \cos 2sZ = \underline{S}_s A_s (e^{2isZ})$$

with $A_s = A_{-s}$ and s now including all integers as well, and equation (1) becomes

$$d^2U/dZ^2 + \underline{S}_s A_s e^{2isZ} U = 0;$$

substitution of (2) for U thus leads to an infinite series of equations of the form

$$\underline{S}_n (2in + \mu)^2 C_{2n} e^{(2in + \mu)Z} + (\underline{S}_s A_s e^{2isZ}) (\underline{S}_{n'} C_{2n'} e^{(2in' + \mu)Z}) = 0$$

Removing the common factor $e^{\mu Z}$ and setting the coefficients of common powers of e to 0 gives another infinite set of equations of the form

$$(3) \quad (\mu + 2in)^2 C_{2n} + \underline{S}_s A_s C_{(2n+2s)} = 0.$$

In the general case for any W of period π if the A_s place limitations on the parameter μ then it is clear that the C_{2n} are also functions of the A_s and thus that the essential nature of the motion is independent of the initial conditions. For the set of equations (3) to be consistent it is necessary that the determinant of the coefficients of the C_{2n} be zero. It can be shown that

- 1) this determinant is convergent;
- 2) that it should converge to zero requires that $\cosh(\pi\mu) = 1 - D(0) \times \sin^2(\pi x (A_0)^{1/2}/2)$
- 3) $D(0)$, the value of the determinant for $\mu=0$, may be approximated by considering the central 3×3 , 5×5 ,

etc., terms to give as close a determination as necessary for an actual value of μ_3 .

To recapitulate, to this point it has been shown that

$$U(Z) = e^{\mu Z} \times \sum_n C_{2n} e^{2inZ}$$

is a solution to equation (1)

and that specifying the A_s determines μ . Substituting $-Z$ for Z in the differential equation does not alter it; therefore

$$U'(Z) = e^{-\mu Z} \times \sum_n C_{2n} e^{-2inZ}$$

is also a solution. Under most circumstances this second solution is independent of the first so that the complete solution is

$$B_1 e^{\mu Z} \times \sum_n C_{2n} e^{2inZ} + B_2 e^{-\mu Z} \times \sum_n C_{2n} e^{-2inZ}$$

with only B_1 and B_2 to be determined by the boundary conditions.

The essential nature of the solution is determined by the parameter μ , with the following possibilities: μ may be real, in which case one part of the solution will increase without bound as Z goes to infinity and the other part will increase without bound as Z goes to negative infinity; μ may be complex, in which case the real part of μ will lead to a similar result; or μ may be purely imaginary, of the form $i\beta$ where β is real. There are several variations in this last case as well. If β is rational, then the complete solution is periodic and bounded; while if β is irrational the solution is aperiodic although bounded. However it is true

although not immediately apparent that when $\mu=i\beta$ with β an integer, U and U' are linearly dependent. The recursion formulas relating the C_{2n} make certain of them equal for certain values of β_4 . For the Hill equation (general W of period π) another periodic bounded solution may exist under these conditions; however for the Mathieu equation ($W=2q\cos 2sZ$, $A_0=a$), a corollary of Ince's theorem noted by Arscott states that when $\mu=i\beta$, β integral, the second independent solution will be of the form

$$B_3 Z U(Z) + F(Z)$$

where $F(Z)$ is a function of period π or 2π , B_3 is a constant having the value $U_2(\pi)/\pi$, and $U(Z)$ is the function given by (2). The term containing Z is unbounded at positive and negative infinity and so the complete solution is unstable in the case of integral β as well.

MATHIEU STABILITY DIAGRAM

For the Mathieu equation the determinant of the coefficients is somewhat simplified; the set of equations is still infinite but there are only three non-zero terms in each equation. As has been indicated above, specific values of a and q determine the characteristic exponent μ and the stability of the complete solution. Recursion relationships derivable from the above equations lead to numerous formulae for approximating μ whose applicability depends on the absolute and relative magnitudes of a and q . For particular a and q values of specific interest, tables of μ have been published making calculation unnecessary.

The parameters (a, q) define a plane which can be divided into regions of stable and unstable solutions to the Mathieu equation; that is regions with imaginary $\mu (=f(a, q))$ and regions with real or complex μ . The boundaries of the regions are known as Mathieu functions of integral order (see figure 3). Considering again the Mathieu equation

$$d^2U/dZ^2 + (a - 2q\cos 2Z)U = 0$$

it is clear that as q approaches 0 there are two solutions to this equation, one of the form $U = \sin \mu Z$ and one of the form $U = \cos \mu Z$, $\mu^2 = a$. The functions $f(a, q)$ with characteristic exponent $i\beta$, β of integral value which reduce to $\sin \mu Z$ and $\cos \mu Z$ when $q=0$ are known as Mathieu functions of the first kind of order μ . A common notation is ce_μ , se_μ , for

cosine-elliptical and sine-elliptical.

The curves in figure 3 show plots of specific values of a and q which lead to solutions to the Mathieu equation the characteristic exponent of which is $i\beta$, β integral. Many interesting properties of these functions have been discovered. For the present purpose it is sufficient to note that the curves do not intersect except at $q=0$ and that when a point (a,q) lies between ce_n and se_{n+1} the value of μ is purely imaginary while between ce_n and se_n , μ may be either complex or real.

Two final facts are necessary to understand the mass-dependent operation of rfq devices. First a and q are directly proportional to U and V , the operating voltages, and inversely proportional to the mass of the ion species in question. For a given U and V the ratio a/q is independent of the mass but the specific values of a and q , and hence the characteristic exponent μ , vary with the mass. Even if the a/q ratio and the mass are fixed, varying the amplitude of U and V changes μ . Second, the symmetries of the Mathieu equation and its solutions are such that if a and q become $-a$ and $-q$, the diagram of stability in figure 3 is simply reflected through the q -axis.

There are regions of the (a,q) plane in which the two sets of regions of stability overlap and other regions in which one or both of the solutions are unstable. As

$$a_x = -a_y \text{ for the mass filter}$$

while

$a_r = -2a_z$ for the ion trap,

for a given U and V there will be some masses confined in either two (filter) or three (trap) dimensions and others for which the ions will eventually leave the device. See figures 4 and 5 for views of the overlapping regions of stability for the mass filter and the ion trap respectively.

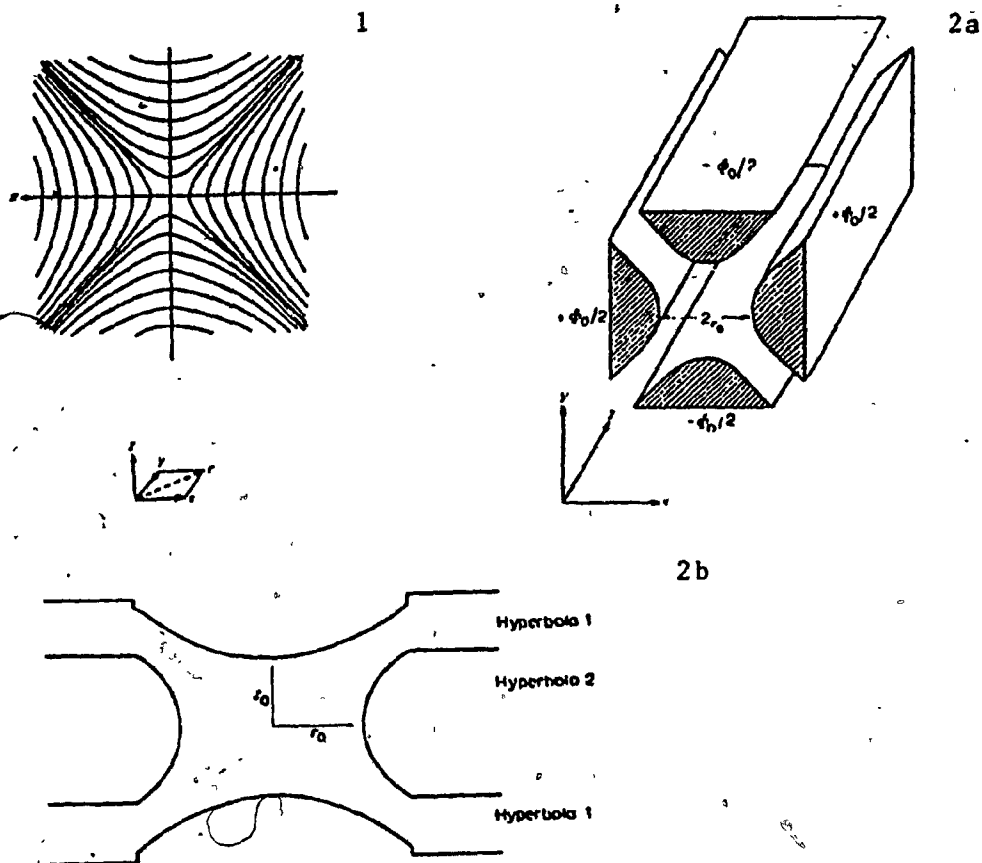


Fig. 1. Equipotential lines for a quadrupole field where $\phi = (\phi_0/2r_0^2)(x^2 - y^2)$.

Fig. 2a. The electrode structure required to generate the potential shown in fig. 1. These are the ideal quadrupole mass filter electrodes having hyperbolic cross-sections.

Fig. 2b. Section through a three-electrode ion trap showing the hyperbolic surfaces employed. The dimensions r_0 and z_0 are related by $r_0^2 = 2z_0^2$.

from Quadrupole Mass Spectrometry
P. Dawson, ed.

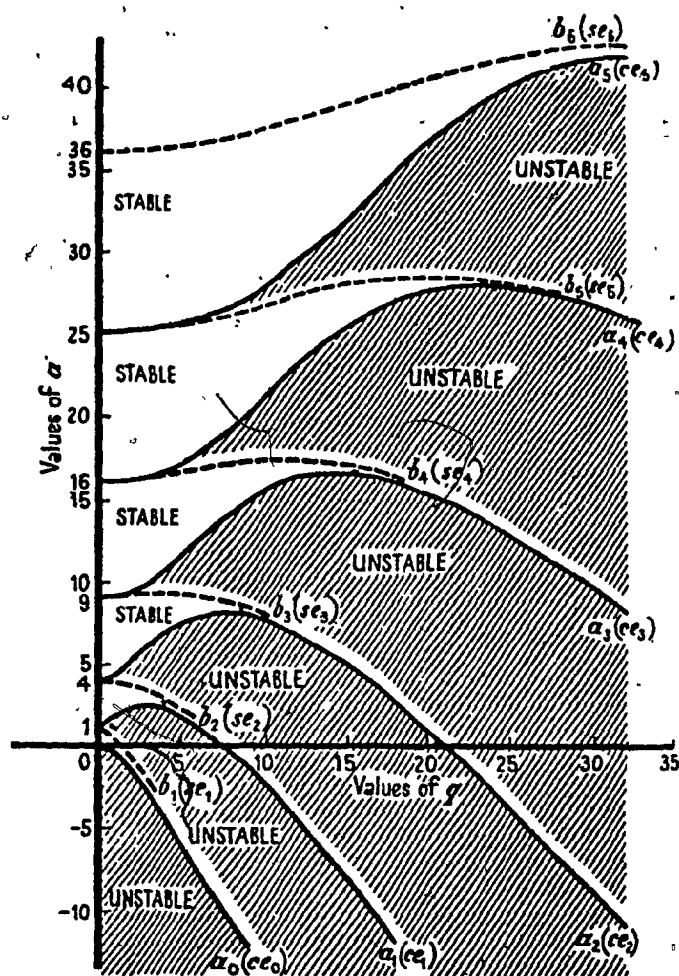


Figure 3. Stability chart for Mathieu functions of integral order. The characteristic curves $a_0, b_1, a_1, b_2, \dots$, divide the plane into regions of stability and instability. The even-order curves are symmetrical, but the odd-order curves are asymmetrical about the a-axis. The complete diagram is symmetrical about the a-axis.

from Theory and Applications of Mathieu Functions
N. W. McLachlan

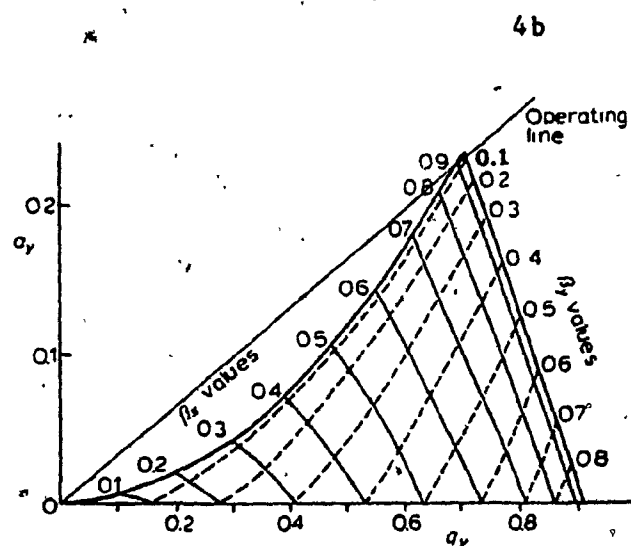
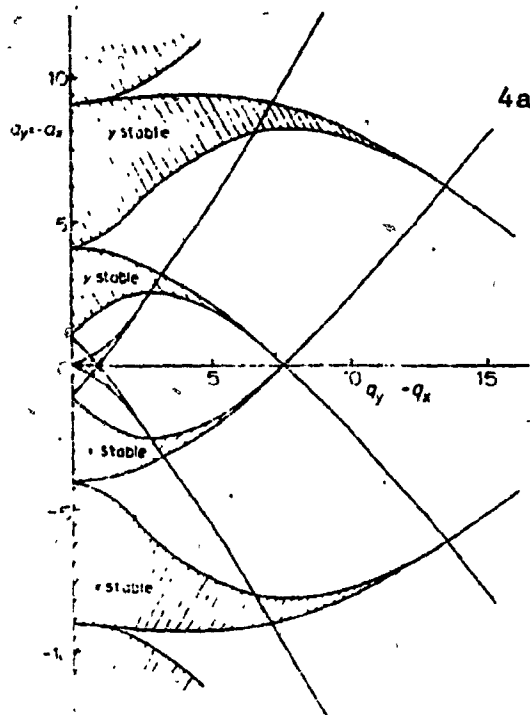


Fig. 4a. The Mathieu stability diagram for the mass filter showing the regions of simultaneous stability in the x and y directions.

Fig. 4b. The lower stability region normally used in mass filter operation showing iso- β lines for the x and y directions and a typical operating line.

from Quadrupole Mass Spectrometry
P. Dawson, ed.

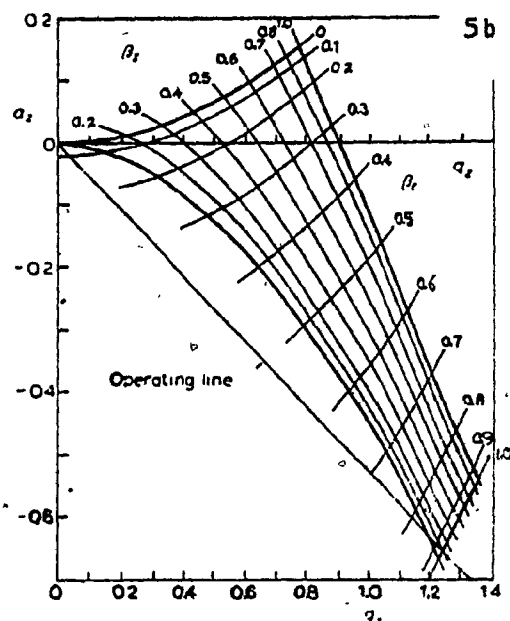
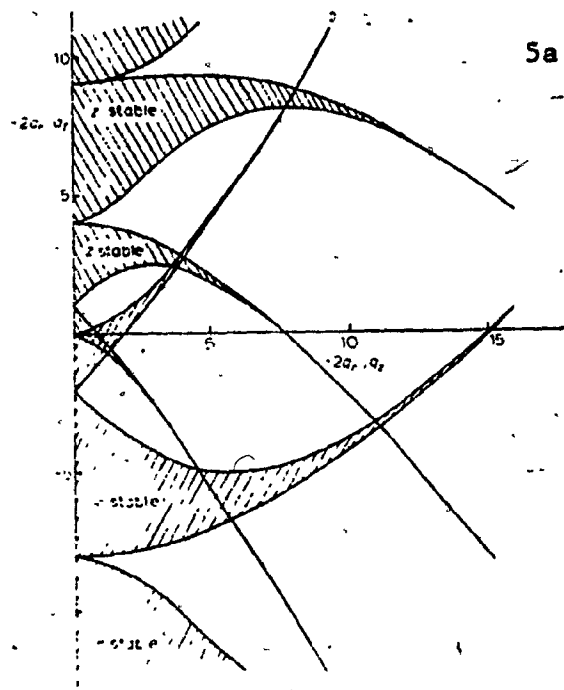


Fig. 5a. The overall stability diagram for the three-dimensional quadrupole ion trap obtained by superimposing stability diagrams for the r and z directions. Fig. 5b. The lowest region of stability for the quadrupole ion trap showing some iso- β lines.

from Quadrupole Mass Spectrometry
P. Dawson, ed.

REFERENCES--II

1. Dawson (see ref. 6, Chapter 1); Chapter 2 of this work gives a description (followed closely in the present work) of potential and electric field derivations and properties as well as the general characteristics of the solutions to the Mathieu equation. Chapter 3 gives a more complete analytical treatment of the general solutions to the equations of motion.
2. See, for example, Mathews and Walker; Mathematical Methods of Physics, 1965, Benjamin and co., New York; pp. 190-192 discuss Floquet's theorem and its applications to Mathieu functions.
3. Morse and Feshbach; Methods of Theoretical Physics, McGraw-Hill, New York, 1953; see pp. 555-568 for a detailed description of solutions to the Mathieu equation including treatment of the Hill determinant.
4. *ibid.*, p. 567
5. Arscott, F.M.; Periodic Differential Equations, MacMillan Co., New York, 1964; PP 34-38 describe Ince's theorem and the consequences for the Mathieu equation solutions if b is integral.
6. McLachlan, N.W.; Theory and Application of Mathieu Functions, Oxford at the Clarendon Press, 1947.
7. See for example Tahir, T; Mathematical Computations 16 (1962), 77; Maeda; Fukada; Sakimura; Mass Spectroscopy in

Tokyo 17 (1969), 530 (referenced by Dawson).

III REAL DEVICES

The analytical solution to the Mathieu equation predicts the motion of a single ion in an ideal trap or mass filter. The solution will be of the form stated above with the stability of the trajectory determined by the parameters U , V , and the charge/mass ratio of the ion in question. These parameters are sufficient to determine the characteristic exponent and the coefficients of the Fourier series in the solution, while the actual amplitude of the motion in a given direction is a function of initial position, velocity, and phase in addition to the C_{2n} .

Even considering the trajectory of a single ion, the analytical approach presents problems. A precise solution depends on knowledge of initial phase, velocity, and position of the ion. These are not always easy to determine and if it is desired to operate the device in question in a continuous mode the amplitudes must be calculated for a large number of different initial phases in order to give a prediction of transmission in the case of the mass filter or capture in the case of the ion trap. Fringing fields in the case of the mass filter and geometrical imperfections in both devices introduce other errors which become very difficult to treat analytically. The existence of other ions and neutral atoms in the vacuum adds further difficulties. It is difficult to even construct an equation which adequately describes the

many-body problem presented. When the equations are formulated, analytical solutions may be difficult if not impossible. The two approaches to the problems presented by actual rfq devices in the real world are numerical solutions and simplified models.

NUMERICAL METHODS--A BRIEF SURVEY

It is not the purpose of this thesis to give a detailed description of numerical techniques brought to bear on the design problems of rfq mass-selective devices but a brief survey of the field is perhaps in order. Real electrode structures do not give rise to perfect quadrupole fields; the technique of finite differences enables a numerical calculation of approximate field strengths which is perhaps more accurate than the perfect quadrupole fields assumed in the Mathieu equation₁. Given a refined field approximation the modified equation of motion may then be integrated point by point to arrive at an ion trajectory based on the time-dependent forces and resultant accelerations. Given initial position and velocity, the position and velocity at a time $t + dt$ are approximated on the basis of weighted averages of velocity and acceleration over dt ₂. A commonly used approximation is the Runge-Kutta method which can give various orders of accuracy of approximation₃. Another numerical method used with success involves matrix multiplication similar to that used by accelerator physicists

to study beam optics. A continuously varying field is broken into piecewise constant portions; the portions are treated as lenses which affect velocity and position in a particular coordinate dimension in a way which can be described by a matrix multiplication; the product of all the matrices which make up a complete cycle of the field gives the single matrix which describes the effect on position and velocity of the traversal of a complete cycle. This matrix raised to the n th power shows the effect of n cycles of the field⁴. Finally the application of phase space dynamics in conjunction with the matrix methods discussed above "not only simplifies long-term trajectory calculations but allows rapid computation of device acceptance for any combination of initial position and initial velocity for the 'ideal' case of an infinitely long sojourn in the rf field."⁵

SIMPLE MODELS OF ION TRAPS AND THE EFFECTS OF SPACE CHARGE

Given the existence of other particles besides the single ion for which the analytical solution is calculated and the field imperfections present in real devices, the Mathieu equation and its solution themselves represent a simplified model of the actual conditions. For the mass filter, particularly when used as a gas analyzer, low ion current densities mean that space charge and the presence of other particles in the filter do not usually constitute a serious perturbation of the equation of motion. However the ion trap

is another matter. The device is intended to accumulate charge and to retain it for long periods of time so that an individual ion is bound to interact with other ions in the trap and with other molecules in the vacuum system. One of the motivations for the research which spawned this thesis was the investigation of injection into a trap of ions created outside the trap. Such ions must clearly have a maximum amplitude in the fundamental harmonic of greater dimensions than the trap unless the trajectory is altered once inside the trap.

In order to determine the capture efficiency of a trap it is necessary to have some notion of the absolute number of ions in the trap at a given time. Most detection methods give a clear picture of relative numbers under given operating conditions. However the absolute magnitude of the stored charge is difficult to estimate. Most published works give estimated values of around $10^7/\text{cm}^3$ for the space charge density^{7,8}. Given the high voltages involved in the confining field a quantitative measurement of this charge collected, for example, on one of the electrodes of the trap presents certain difficulties in instrumentation. Some investigators have built essentially transparent traps and collected the ions ejected from the traps on electron-multiplier dynodes⁶, but there are enough variables in the transfer efficiency from trap to multiplier to make this method of questionable precision. Fischer⁷ and

Dehmelt⁸ have offered two different methods of estimating the maximum number of ions contained in a trap based on simple models of the ion motion while R. B. Moore has suggested to the author a means of relating the amplitude of the ion signal produced by the non-destructive detection means employed to the charge and hence the number of ions present in the trap.

FISCHER'S MODEL

The method of Fischer⁷ assumes that the buildup of space charge in the trap has the effect of changing the dc bias voltage U in the Mathieu equation. Based on the potential distribution inside an elliptical spheroid of constant charge density ρ with $r_0^2 = 2z_0^2$ he derives the result that $dU_z = -dU_r = -\rho r_0^2 / 4\epsilon_0$ where ϵ_0 is the permittivity of free space. The shift in dc bias dU will lead to a change in the characteristic exponent and thus to a shift in the resonant frequency of the ions which may be measured with the detection circuitry employed. In practice the shift in dU is measured directly as the lateral translation of the ion peak as its amplitude grows.

THE DEHMELT-WUERKER-MAJOR MODEL

The theoretical model of ion trapping attributed by Dawson to Dehmelt et al¹¹ starts from the equation of motion, makes some assumptions about that motion, and goes on to derive an equivalent parabolic potential well in which an

individual ion would execute simple harmonic motion. Further assumptions about the average distribution of ions in a filled trap lead to an estimate of the maximum charge density acceptable. This model is worth examining in some detail because it gives a picture of the confinement process which is a little easier to cope with intuitively than the Mathieu equation solutions.

The method of Dehmelt, Major and Wuerker^{8,9,10} breaks the motion of an ion in the trap into a micromotion which may be described as an oscillation around a moving center at the frequency of the rf drive and a larger motion, that of the center around which the micromotion oscillates. The assumptions are that the micromotion amplitude is much smaller than that of the drift motion but that the velocity of the micromotion is much greater than that of the drift. Based on these assumptions an equation describing the drift motion is derived which describes a particle of the same charge/mass ratio moving in a parabolic potential well, that is an equation of simple harmonic motion. The frequency of this motion turns out to be roughly the same as that predicted by the characteristic exponent.

One starts, then, from the equation of motion put in the canonical Mathieu form:

$$d^2n/dx^2 = -(a_n - 2q_n \cos 2x)n \text{ with } x = \omega_{rf}t/2,$$

where $n = r$ or z and a_r and a_z are as previously defined.

Assume

$$n = Z + z,$$

where Z is a large-scale secular motion and z is a micromotion due to the rf drive and oscillatory about Z

Assume that the driving force, proportional to q , is not too large so that $z \ll Z$ but $dz/dt \gg dZ/dt$. Then

$$d^2 z/dx^2 = -(a_n - 2q_n \cos 2x)Z$$

If $a \ll q$ and Z is constant through one rf cycle, integration yields

$$z = -(q_n Z \cos 2x)/2,$$

an intermediate result regarding which it is interesting to note that the micromotion increases with Z and is 180° out of phase with the rf drive. Substitution into the equation which relates n , Z , and z yields

$$n = Z - (q_n Z \cos 2x)/2$$

and substitution of this result into the original equation leads to

$$d^2 n/dx^2 = -a_n Z + (a_n q_n Z \cos 2x)/2 + 2q_n Z \cos 2x - q_n^2 Z \cos^2 2x$$

which when integrated over a complete cycle of the rf drive yields the result that

$$(d^2 Z/dx^2)_{av} = -(a_n + q_n^2/2)Z, \text{ as } (d^2 Z/dx^2)_{av} = 0.$$

The above is the equation for simple harmonic motion with angular frequency with respect to the variable x of $\omega_x = (a_n + q_n^2/2)^{1/2}$. Remembering that $x = \omega_{rf} t/2$, the ionic

oscillation angular frequency with respect to time is

$$\omega_{ion} = \beta \omega_{rf}/2 \text{ with } \beta = \omega_x.$$

Consider motion in the z direction, with $a_z = 0$, $q_z = -2eV/mz_o^2 \omega_{rf}^2$. The modified equation of motion then becomes

$$d^2Z/dt^2 = -(e^2V^2/2m^2z_o^4 \omega_{rf}^2)Z.$$

The "force" on an ion of mass m and charge e is therefore given by

$$md^2Z/dt^2 = -eD_z/dZ, \text{ with}$$

$$dD_z/dZ = eV^2Z/2mz_o^4 \omega_{rf}^2. \text{ Integrating } dD \text{ from } 0 \text{ to } z_o,$$

$$D_z = eV^2/4mz_o^4 \omega_{rf}^2.$$

Keeping in mind the relationships between r_o and z_o and between q_r and q_z , it is easily established that $D_r = D_z/2$ for a trap with $r_o^2 = 2z_o^2$.

The assumptions of small q , negligible a , slowly varying Z and $z \ll Z$ thus lead to a picture of an ion executing simple harmonic motion in a "pseudopotential" well parabolic in shape and of depth D_n . According to Wuerker¹⁸ these assumptions remain self-consistent up until a point around $q=.4$ when the ratio z/Z becomes too large to support the arguments. Dawson further points out that the effect of an additional dc bias (non-zero a) changes the well depth depending on its sign so that a point is eventually reached in either the z or r direction at which the ion is no longer bound¹¹.

It is clear that for an ion to experience the force due

to this pseudopotential it must be moving in the trap. A stationary ion would feel a force the ac component of which would average to zero and the dc component of which would be simply due to the dc bias voltage. It is also true that every ion added to the trap must modify the fields experienced by those already in the trap and that the picture of a single ion executing large-amplitude simple harmonic motion cannot adequately describe the behavior of individual ions in an ion cloud contained within a trap. There is some evidence that the ions in an ion cloud become "crystallized", particularly in the presence of a buffer gas, and that except for the micromotion due to the rf drive they remain relatively stationary₁₈ (see figure 6a,b). The force averaged over the rf drive cycle then gives rise to the confining force.

An estimate of the space charge-limited maximum density of ions in the trap may then be made based on the assumption that within the ion cloud the potential must be constant or the ions would redistribute themselves. Thus if P_p is the pseudopotential derived above and P_e is the electrostatic potential due to the charge of the ions in the trap, then

$$P_p + P_e = \text{constant such that}$$

$$-\text{div. grad } P_e = \text{div. grad } P_p = 4\pi\rho_{\text{max}}$$

with ρ_{max} the maximum charge density.

Making use of the relationships between D_z and D_r and between r_0 and z_0 , if there is no dc bias then the pseudopotential

P_p may be expressed in the form

$$P_p = (D_z/4z_o^2)(x^2 + y^2 + 4z^2) \text{ so that}$$

$$\text{div.grad}P_p = 3D_z/z_o^2;$$

in view of the above one thus has

$$\rho_{\text{max}} = 3D_z/4\pi z_o^2.$$

AN EMPIRICAL MODEL

R. Moore has suggested to the author that it should be possible to relate the amplitude of the detected signal to the absolute number of the ions in the trap. An oscillating body driven into periodic motion in a damping environment dissipates an amount of energy related to the driving force and frequency, the amplitude of the oscillation, and the damping force acting on the body; if these parameters can be determined for a given ion the power dissipation per ion can be determined. If the motion of each ion is more or less the same and if the total power input into the system can be determined then the number of ions can be ascertained.

The ion detection system employed involved application of a low-amplitude detection drive frequency across the endcaps of the trap which were part of the capacitive load of a high-Q resonant circuit. The fundamental ion oscillation frequency was varied while the amplitude of the detection drive voltage across the endcaps was monitored. A drop in the detection voltage amplitude indicated a change in the "Q" of the tuned circuit due to absorption of energy by the ions

at the resonant frequency.

As mentioned above¹⁸, there is a certain amount of evidence for the validity of the assumption that the ions, when in a cloud damped by the presence of a buffer gas, become "crystallized" into a more or less stationary array in which the bound ions execute the micromotion described by the Dehmelt model. There is perhaps less evidence to support the assumption of constant charge density. Results of Knight and Prior¹² and Schaaf, Schmeling and Werth¹³ suggest that the charge distribution is an elliptical spheroid with the radial density function gaussian in shape; the charge is mainly confined to a region with axes around $1/6$ the length of z_0 and r_0 in the z and r directions respectively. If the field between the endcaps is approximated by the field between parallel plates spaced $2z_0$ apart then the driving force may be approximated by $f \cos \omega_{dr} t$. The fundamental oscillation frequency of the cloud, the ω_{ion} predicted by Dehmelt, proves to be reasonably close to the actual frequency at which the ions do absorb energy from the detection circuitry.

A fair amount of work has been done on the effects of collisions with assorted neutral species on the trajectories of ions in traps. Briefly, for light background atoms the energy loss per collision is proportional to the original energy of the incident ion and the constant of proportionality is directly related to the ratio of the respective masses while the number of collisions per unit

time is proportional to the velocity of the ion₁₄. A damping coefficient constructed from this sort of energy loss mechanism gives rise to a term proportional to the square of the velocity and thus to a nonlinear differential equation. If the damping term is small a common way of treating such nonlinear terms is to construct a linear term which results in the same average energy loss over one cycle and then to solve the linear equation which results₁₅. However attempts to derive a suitable damping term on the basis of geometric cross-sections and mean free paths resulted in damping coefficients which led to calculated amplitudes of oscillation on the order of meters; instead of a damping term based on first principles it was necessary to derive a term from an experimental measurement of the peak width, an extrapolation on the basis of the relation between dc bias voltage and ion oscillation frequency which yielded a "Q" for the assumed damped resonant circuit, and a calculation of the damping factor based on the relationship between Q and the damping coefficient. It seems likely that the motion of the ions under the influence of the rf drive field increases the effective cross-sectional area in some way.

The basic differential equation chosen to describe the ions under the influence of the detection drive was

$$d^2z/dt^2 + (R/m)dz/dt + \omega_{ion}^2 z = F \cos \omega t / m$$

with $F = eV_{det}/z_0$,

the solution to which may be found in many elementary physics

or mathematics books₁₆ to be

$$z = (F \cos(\omega t - \theta)) / (m^2(\omega_{ion}^2 - \omega^2)^2 + \omega^2 R^2)^{1/2}$$

$$\tan \theta = \omega R / (\omega_{ion}^2 - \omega^2).$$

For a driven damped system the free resonant frequency, the damped resonant frequency, the frequency at which the driven oscillations reach maximum amplitude and the frequency at which maximum power is dissipated are not all the same. However if the damping factor is small they are very close and may be considered equivalent. These approximations lead to

$$Q = m\omega_{ion}/R$$

$$A_{max} = F/\omega_{ion}R = eV/\omega_{ion}R$$

The energy input to the resonant circuit per unit time may be expressed as

$$\omega C V^2 / 2Q_{res};$$

the power dissipated by the ions is

$$N\omega(m\omega^2 A^2 / 2Q_{ion}).$$

Assuming the energy input into the resonant circuit to be unchanged, the change in amplitude in the resonant circuit must be balanced by the energy absorbed by the ions:

$$\omega C V^2 / 2Q_{res} = \omega C V'^2 / 2Q_{res} + N\omega^3 m A^2 / 2Q_{ion}.$$

Substituting for A and solving for N,

$$(V^2 \omega C / 2V'^2 Q_{res} - \omega C / 2Q_{res})(\omega m z_0^2 / e^2 Q_{ion}) = N$$

In fact the constant power assumption is not valid. All one can say with certainty is that the power dissipated at V' is $\omega C V'^2 / 2Q_{res}$ while that dissipated in the tank circuit is

$\omega C V'^2 / 2Q_{res}$, with Q and Q' the effective Q of the tank circuit without and with the coupled ions. Setting the difference equal to the power dissipated by the ions,

$$(Ne^2 V'^2 Q_{ion}) / \omega m z_o^2 = (\omega C V'^2) / 2 \times (1/Q'_{res} - 1/Q_{res})$$

$$\text{or } N = (C \omega^2 m z_o^2) / (2e^2 Q_{ion}) \times (1/Q'_{res} - 1/Q_{res})$$

or if $Q' = Q + dQ$ then to terms in dQ^2 ,

$$N = (C \omega^2 m z_o^2) / (2e^2 Q_{res} Q_{ion}) \times (dQ/Q).$$

Comparing this with the constant power assumption one finds that the two are identical except that in the constant power case the term (dQ/Q) is replaced by $(V^2/V'^2 - 1)$ which, if dV is small, is approximately equal to $d(V^2)/V^2$. If R is the isolating resistor between the detection drive and the tank circuit, V_o is the detection oscillator amplitude, V and V' are the voltages developed across the detection tank circuit, and $Q/\omega C$ is the effective resistance of the tank circuit at resonance, then

$$V = V_o Q / (R\omega C + Q)$$

$$V' = V_o Q' / (R\omega C + Q')$$

If $R \gg Q/\omega C$ then

$$V'^2/V^2 = (Q'^2/Q^2) \times (1 - 2Q'/R\omega C)(1 + 2Q/R\omega C)$$

and finally

$$d(V^2)/V^2 = 2dQ/Q$$

if $dQ/Q \gg dQ/R\omega C$, so that

$$\begin{aligned} N &= (V_o^2 \omega C / 2V'^2 Q_{res} - \omega C / 2Q_{res}) (\omega m z_o^2 / 2e^2 Q_{ion}) \\ &= (d(V^2)/V^2) (C \omega^2 m z_o^2 / 4e^2 Q_{res} Q_{ion}) \end{aligned}$$

CAPTURE-LOSS RATE LAW

The rate of change of ions in the trap will be affected by the number of ions in the trap, the number of neutral atoms or molecules in the trap, and the rate at which ions are being formed in or introduced into the trap. Dawson¹⁷ suggests a rate law of the form

$$dN/dt = k_1 p - (k_2 N^2 + k_3 N p)$$

with N the number of ions in the trap, p the pressure of the background gas, k_1 a constant related to the rate of formation of ions, k_2 to the rate of loss of ions from the trap due to collisions with other ions and k_3 to the rate of loss from collisions with molecules of the background gas. Dawson's formula is designed for ions formed by ionization of gas already in the trap. For the condition in which an ion current is injected into a trap filled with a buffer gas, it is still reasonable to assume that the capture rate will be proportional to the pressure of the buffer gas. Thus if the ion current remains constant the above law should still apply. The constants may be evaluated through some simple experiments.

With the trap saturated, the losses equal the rate of capture:

$$k_1 p = k_2 N_s^2 + k_3 N_s p \text{ when } dN/dt = 0.$$

If the trap is emptied and the ion source turned on, while N is small

$$dN/dt = k_1 p.$$

while if the trap is filled and the source turned off,

$$dN/dt = -(k_2N^2 + k_3Np)$$

which integrates to

$$(1/k_3p) \log_n((k_2N + k_3p)/N) = t. + \text{constant.}$$

Assuming $N = N_0$ at $t = 0$ this expression may be put in the form

$$1/N = ((k_3p + k_2N_0)/k_3pN_0) \exp(k_3pt) - k_2/k_3p$$

which is of the general form $y = a \exp(bc) + c$ and thus can be treated by standard exponential curve-fitting procedure using the decay data plotted as $1/N$ vs. t .

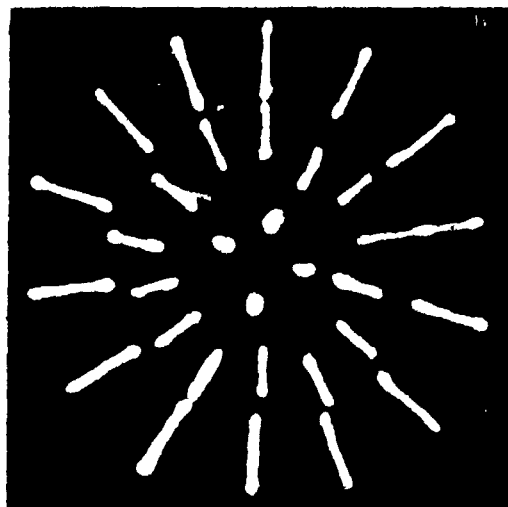
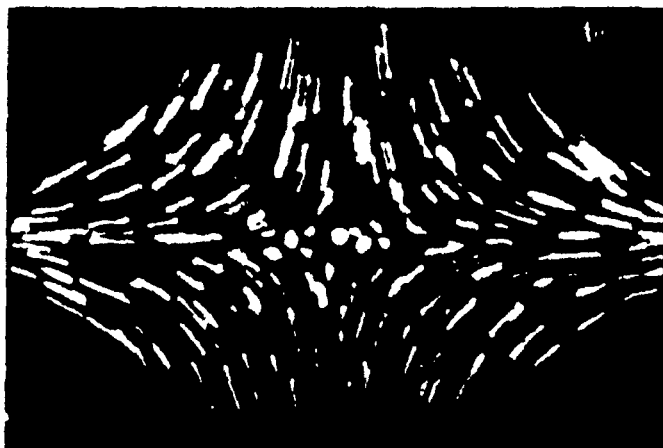


Fig. 6a. Many body suspension, viewed in the r - z plane. Experimental values: $V_{ac}=500V_{rms}$, drive frequency=210 Hz, particle oscillation frequency=21.7 Hz.
Fig. 6b. Suspension of 32 positively charged particles viewed in the r - θ plane. $V_{ac}=500V_{rms}$, drive freq.=135 Hz, oscillation freq.=43.6 Hz, $e/m=.00765\text{coul/kg}$.

from Wuerker, Shelton, Langmuir;
Journal of Applied Physics 30 (1959), p. 342

REFERENCES--III

1. * See Binns, K.; Lawrenson, P.; Analysis and Computation of Electric and Magnetic Field Problems, Pergamon, Toronto, 1973, pp.241-289 (Chapter 11) for a concise description of the method of finite differences.
2. A short description of different methods of numerical integration may be found in Mathews and Walker (see ref.2, chapter 2), pp.331 338.
3. Prescriptions for specific applications of this and other methods can be found in Bronson, R.; Modern Introductory Differential Equations, McGraw-Hill, 1973, Chapters 32-36.
4. See Steffen, K.; High Energy Beam Optics, Interscience publishers, 1964. Chapter 1 covers basic Quadrupole optics while Chapter 4 deals with a phase space approach. Also see Dawson, P.; "A Detailed Study of the Quadrupole Mass Filter", International Journal of Mass Spectrometry and Ion Physics 14 (1974), pp.317-337 for applications to the mass filter including fringing fields.
5. Dawson, P. (ref.6, chapter 1), p. 91.
6. Dawson, P.; Whetten, N.; Naturwissenschaften 56 (1969), p.109.
7. Fischer; Z. Phys. 156 (1959), p. 26.
8. Dehmelt, H.; "Radio Frequency Spectroscopy of Stored Ions I: Storage", Advances in Atomic and Molecular Physics 3 (1967), pp. 53 ff.

9. Wuerker, R.; Goldenberg, H.; Langmuir, R.; Journal of Applied Physics 30 (1959), P. 441.
10. Major, F.; Dehmelt, H.; Physical Review 170 (1968), p. 91.
11. Dawson (see ref. 6 chapter 1), p. 213.
12. Knight, R.; Prior, M.; "Laser/scanning measurement of the density distribution of confined ${}^6\text{Li}^+$ ions", Journal of Applied Physics 50(5) (1979), pp. 3044-3049.
13. Shaaf, H.; Schmeling, U.; Werth, G.; "Trapped Ion Density Distribution in the Presence of He-Buffer Gas", Applied Physics 25 (1981), pp. 249-251.
14. Dehmelt; Major; (ref. 10 above).
15. Kryloff, N.; Bogoliuboff, N.; Introduction to Non-Linear Mechanics, Princeton University Press, 1947. See chapters 3,5.
16. See, for example, Becker, R.; Introduction to Theoretical Mechanics, McGraw-Hill, New York, 1954, pp144-151.
17. Dawson, (ref. 11 above), pp. 207-210.
18. Wuerker, R.; Shelton; Langmuir, R.; Journal of Applied Physics 30 (1959), P. 342.

IV EXPERIMENTAL PROCEDURE AND RESULTS

APPARATUS

The experimental setup described in this thesis may be conveniently divided into five main parts. These are the vacuum system, the ion gun assembly, the mass filter and its associated detection system and power supply, the ion trap and its detection system and power supply, and the computer interface system.

VACUUM SYSTEM

The main components of the vacuum system were a Leybold-Heraeus 230 litres/second turbomolecular pump and power supply and an Alcatel 2012 rotary-vane two-stage roughing pump which were used to evacuate the chambers in which the trap and mass filter were operated. Forepressure was monitored by a thermocouple gauge while chamber pressures were measured in the mass filter experiments with a Penning-style ionization gauge and in the ion trap system with a Spectrum Scientific Ltd. SM 800A residual gas analyzer. The volume of the mass filter chamber was approximately 10.3 litres (630 in³); that of the ion trap, about 11.8 litres (715 in³). A 30cm section of 10cm diameter aluminum tube was common to both chambers. The remainder of the trap chamber was predominantly stainless steel while many of the tubes in

the mass filter system were aluminum. Vacuum seals were of the O-ring type. Most of the rings in the trap system were Viton while the mass filter was put together using Buna-N rings. Feed-throughs for electrical connections were glued in place with vacuum epoxy for the mass filter system while for the trap welded ceramic-insulated feedthroughs were employed. The trap system had two further special features: a liquid nitrogen cold finger and a needle-valve controlled helium leak which permitted regulation of the background pressure. (See figure 7 for a block diagram of the two systems.)

Testing of the mass filter did not proceed beyond a fairly rudimentary stage; vacuum requirements were not very stringent and it is sufficient to note that the system operated in the range of 10^{-5} - 10^{-6} Torr with the ion gun at a moderate current level. After the gun had been operated for around 45 minutes the pressure began to increase, perhaps due to heating of the O-rings, and it would become necessary to shut the gun heater down and allow the system to cool off before continuing. No effort was made to ascertain the constituents of the residual gas.

In the case of the ion trap a low background pressure is essential to attain good confinement times. Some effort was made to bake the chamber, both with electric heating tape and with a heat gun, although it is doubtful that temperatures higher than 100°C were attained. Addition of the liquid

nitrogen cold finger resulted in a substantial reduction of the base pressures. After baking, pressures of 5×10^{-8} Torr were routinely measured with the quadrupole gas analyzer; at higher pressures the analyzer readings were roughly equivalent to those of the Penning gauge which was used as a check on the calibration of the RGA. Principal components of the residual gas at the base pressure were water vapor and nitrogen. There were some traces of hydrocarbons although these were a small fraction of the total.

Measurement of the buffer gas pressure when a significant amount of helium had been leaked into the chamber presented a problem as the sensitivity of the gas analyzer to high helium pressures seemed to decrease with time. An attempt to correlate compression ratio of the turbo pump and forepressure as measured with the thermocouple gauge with the readings of the gas analyzer, taking into account the factor of 4 introduced by the relative sensitivity of the analyzer to helium and its calibration for nitrogen, showed rough initial agreement between the two methods. However as time passed the reading of the gas analyzer would decrease markedly while the forepressure would remain constant. (A possible explanation offered by L. Nikkinen is that the pressures of helium might be high enough to cool the filament in the analyzer significantly, thus reducing the electron emission and thus the ion current.) The author feels that agreement of the initial reading of the gas analyzer with the

forepressure calculation gives a background pressure accurate at least to within an order of magnitude.

ION GUN

The basic design for the ion gun, together with the principal components and a supply of cesium and rubidium ammunition were brought by R. Moore from researchers at the University of Mainz, W. Germany, where such sources are routinely employed₁. The basic principles of operation are as follows.

Zeolite, a sodium aluminosilicate ($\text{Na}_2(\text{Al}_2\text{Si}_4\text{O}_{12})$) commonly used as a molecular sieve, can be considered as an aluminosilicate base with two very loosely bound alkali metal ions. When the substance is heated, the alkali ions will leave the substance, always as ions and never as neutral atoms. If the sodium zeolite is treated by an ion exchange process in a saturated solution of another soluble alkali salt (e.g., CsCl), a Cesium aluminosilicate is produced which will when heated give off cesium ions. Weber and Cordes₂ refer to an ion source constructed of cesium zeolite which produced ion currents of on the order of 10 microamperes over a lifetime in excess of 300 hours of operation.

In order to take advantage of the above properties the zeolite was placed in a stainless steel cylinder with a small orifice (hole) in one end and a threaded plug in the other. A stainless steel electrode spotwelded to the plug provided

an electrical contact to bias the gun. The gun was placed in a boron nitride cylinder the exterior of which was threaded with a pitch of 10 threads per mm; the grooves helped maintain the spacing of a .25 mm tungsten filament which was wrapped around the boron nitride to provide heating. A Macor (Corning machinable ceramic) jacket enclosed the tungsten-wrapped boron nitride oven. Thus the boron nitride provided electrical insulation between the gun and the filament while the Macor provided thermal and electrical insulation between the filament and the auxiliary support structure. (See figure 8 for details of the construction of the ion gun.)

Two separate steel cylinders were employed to contain the zeolite. One was an ordinary cylinder as described above; the other had the orifice partially blocked with tungsten wires to reduce the emission of neutral atoms which might be deposited on the steel walls and then reejected. No difference in performance was noted between the two guns. Two separate types of ion-exchanged zeolite were employed: cesium and rubidium. No efforts were made to quantify the differing properties of the two types of source although it seemed that higher currents at lower temperatures were produced by the cesium than by the rubidium zeolite. A mixture of the two substances produced an ion beam which could be decomposed into two separate peaks of mass ratio roughly $2/3$ by the mass filter described later. The cesium

ion source was studied a bit more thoroughly as it was employed both for the mass filter and the ion trap. An optical pyrometer indicated that at around 700°C the gun began to emit a detectable current. The gun was operated over a wide range of heater currents and produced an ion current of in excess of 1 microampere measured with a faraday cup and a picoammeter. A circuit was constructed whereby the gun could be biased negatively with respect to ground through a large resistor and then pulsed about 15 volts positive with a square pulse through a capacitor; pulse widths of as short as several microseconds were distinguishable in the output of the mass filter measured with an electron multiplier tube.

MASS FILTER


The design process which resulted in the mass filter could kindly be described as pragmatic. Half-inch diameter stainless steel rods were chosen as there was some half-inch stock in the machine shop; the operating frequency of one Mhz was chosen because the author had a crystal and some experience with oscillators at that frequency; the length of six inches was a compromise between resolution and ease of manipulation. The length, diameter, and frequency were checked with empirical formulae given in Dawson and found to require an rf drive voltage of less than 1000Vp-p whereupon construction was started. Two problems, mechanical precision and voltage regulation, were encountered.

The literature contains many ingenious methods to ensure precise alignment of the rods and many caveats stressing the importance of precise alignment in order to achieve good resolution₃. Faced with an abundance of low-precision .95 cm diameter ceramic insulators and a relative dearth of 1.27 cm ruby spheres, the author chose to design a supporting structure which would allow alignment of the rods after assembly rather than depending on precise machining to achieve the tolerances necessary for high resolution. Accordingly the rods were attached at each end to ceramic insulators which were recessed into large holes in aluminum endplates and bolted through holes larger than the bolts, with teflon washers providing a friction lock. Three of the rods were adjustable in two directions; brass screws of pitch of 10 threads/mm, with steel ball bearings pressed into the ends, were brought to bear on the sides of the ceramic insulators. It proved relatively easy to adjust the alignment of the rods to within .025 mm tolerance. It also proved relatively easy to break the ceramic insulators. The whole assembly was mounted in a 10 cm diameter aluminum tube in the walls of which were glued two Kovar feedthroughs which provided electrical contacts for the electrical drive for the rods. (For details see figure 9.)

The power supply presented three main problems: achieving the high voltage required, maintaining the ac-dc ratio to a high degree of precision, and balancing the output

to maintain zero potential along the center axis. This last condition is particularly difficult to achieve with any degree of certainty as any probe attached to one side of the power supply will load that side. The technique finally employed was measurement with a high voltage high impedance probe attached first to one side and then the other; although the load unbalanced the high-Q drive circuit, when the effect was the same on both sides it was assumed that the circuit was effectively balanced.

The rf drive was provided by an adjustable signal generator amplified by a broad-band rf amplifier with a maximum output of 25Vp-p. In order to step this up to 1000V a transformer was required with a turns ratio of 40/1. The 1Mhz operating frequency and the stray capacitance of on the order of 50pf dictated the employment of air-core transformers in order to achieve low enough inductance to tune the secondary. Shielding was necessary to eliminate feedback coupling the air-core transformer to the input of the rf amplifier. Tuning capacitors, a balancing capacitor, a capacitive divider used to pick off a low-amplitude signal proportional to the ac signal, and the mass filter itself coupled capacitively to the ac transformer and through a dual 3 megohm film resistor ladder to the dc bias source, made up the secondary load. AC drive amplitudes in excess of 1000Vp-p were achieved before arcing occurred in the tuning capacitors. See figure 10 for a block diagram of the mass



filter system.

The standard means for achieving stable ac/dc ratios in high-resolution applications involves the use of vacuum tube diode rectifiers₅; the author felt that for preliminary test purposes an op-amp assisted signal diode rectifier would be easier to implement. Accordingly such a circuit was built using a 318 fast op-amp and a germanium diode to minimize errors due to forward-bias drop and switching times₆. The circuit proved considerably more linear than the diode itself although at very large and very small voltages some irregularities manifested themselves. 1 Mhz appeared to be the limit of the circuit constructed although perhaps better diodes and faster op-amps exist which might push this limit a bit higher. The output of the capacitor-divided rectified ac signal was fed to a variable-gain dual-polarity dc amplifier which produced positive and negative voltages of 0-100 volts proportional to the ac signal₇. These voltages were then coupled resistively to the rod pairs. See figure 11 for a circuit diagram of the d.c. power supply.

EXPERIMENTAL RESULTS

The mass filter was primarily used as a test bed for the ion gun and the electronic circuitry needed to drive the devices. Although the power supply for the mass filter was slightly more complicated than that of the trap, the injection of ions into the mass filter was trivial while

there was some doubt as to whether injection into a trap was possible, let alone feasible. Detection of the ions was accomplished with existing previously utilized apparatus in the case of the mass filter while the resonant detection circuitry was untested and built specially for the ion trap. Hard data from the mass-filter experiments is minimal and of little general interest. However a qualitative description of the results obtained is in order.

The mass filter was mounted coaxially with the ion gun and an electron multiplier (RCA 4643-4B). The ion gun was charged with a mixture of cesium and rubidium zeolite. First the dc voltages were turned off and the ac voltage was increased monotonically while the ion gun was maintained at a constant heater current and with a constant bias voltage of 18 volts. It was observed that as the ac voltage increased from zero, the ion current first increased rapidly, then fluctuated over a wide range of ac values, and finally diminished to zero past a particular threshold voltage. Second the ac voltage was set to a point slightly below the cutoff point and the dc bias was increased until the signal disappeared. The dc and ac voltages were adjusted at this point until a narrow peak of transmission occurred; then the voltages were decreased, with the ac/dc ratio remaining constant. It was observed that another region of transmission occurred at a voltage amplitude of about $2/3$ that of the maximum region. Up to this point the multiplier

currents had been measured with a dc picoammeter. A final experiment performed involved the operation of the mass filter in the ac-only mode and the introduction of a resistor-capacitor circuit which enabled the gun to be biased negatively and pulsed positively with a square pulse of variable width. The output of the multiplier was monitored with an oscilloscope connected across a 100-ohm resistor to give a low time-constant. There was no discernible current when the gun was biased negatively. Positive pulses as narrow as 3 microseconds produced a definite pulse output from the multiplier.

ION TRAP

David Lunney of McGill's Electrical Engineering department, assisted by R. Moore, was responsible for the design and construction of the ion trap. A fuller description of design and construction considerations will appear in Lunney's Master's thesis; a brief synopsis of the relevant considerations follows.

An r_0 was chosen which would be large enough to contain a significant number of ions and small enough that the voltages required would not be too high and that the overall dimensions of the trap would be convenient. It was originally planned to use barium as a test ion due to its optical properties and the possibilities of using a laser

fluorescence detection system. However, an ion-resonant electromagnetic detection scheme proved easier to implement. The detection circuitry was designed around an ion resonant frequency of about 50 kHz with no dc bias. Given the approximate relation

$$\omega_{ion} = q_z \omega_{rf} / (2)^{3/2} \text{ with}$$

$$q_z = 2eV / m z_o^2 \omega_{rf}^2$$

fixing r_o , m , and ω_{ion} leaves V and ω_{rf} as variables. It was possible using a Mountain Computer Inc. ADC-DAC digital-to-analog interface with an Apple II+ microcomputer to sweep over $\pm 5V$ without additional hardware. Lunney's calculations showed that this would result in a variation in the ion oscillation frequency over the range of 49-55 kHz. Varying the ac amplitude made it possible to put the resonant interaction of the ions with the detection circuitry at about the middle of the dc sweep. Ions from the ion gun were injected through a hole bored in one of the end caps of the trap. (See figure 12 for details of the trap construction; figures 13 and 14 are photographs of the overall experimental setup and a detail showing the hole in the end cap electrode.)

RESONANT DETECTION SYSTEM

The detection system employed utilizes the coupling of the ions to a highly tuned tank circuit containing the two

end caps of the trap as part of the capacitance. Similar circuits have been employed in the past, notably by Fischer₈, who gets early credit for the technique along with Berkling₉, and Rettinghaus₁₀. The ions, as mentioned before, have a fundamental oscillation frequency ω_{ion} which is a function of the charge/mass ratio, the rf drive frequency and amplitude, the dc bias, and the dimensions of the trap. When ions are present in the trap and ω_{ion} is the same as the resonant frequency of the tank circuit there may be an exchange of energy between the ions and the tank circuit. Under certain circumstances the tank circuit will take energy from the ions, cooling their oscillation. However, if the tank circuit is driven externally and the motion of the ions is damped by a light buffer gas, the effect is to lower the "Q" of the tank circuit and thus the amplitude of the oscillations therein₁₁. As ω_{ion} is a function of the dc bias voltage applied between the endcaps and ring electrode, varying this voltage will sweep the ion frequency over a certain range; if the frequency sweep includes the frequency to which the tank circuit is tuned, work is done on the damped ions and a dip in the voltage across the endcaps occurs which can be observed with suitable circuitry.

The detection circuitry was modeled after a similar circuit₁₂ modified to suit the present purposes. The coil which makes up the inductive part of the tank circuit is loosely coupled inductively to a fast integrated buffer

followed by a high-gain rf transistor amplifier. The input of this amplifier was bypassed with an LC shunt to reduce the amplitude of the rf drive reaching the detector. The amplifier is followed by an emitter-follower buffer and a rectifier stage which derives a dc signal from the ac input. Both the buffered rf amplifier and the detector output may be monitored. The amplifier output gives some idea of the absolute amplitude of the oscillations in the tank circuit while the detector output shows changes to this amplitude as peaks and valleys. The tank circuit is driven by a signal generator tuned to the resonant frequency and coupled through a three megohm film resistor. (See figure 15.)

DATA ACQUISITION SYSTEM

Data from the experiments performed using the ion trap were stored on floppy discs using the Apple II+ computer and the Mountain Computer Inc. ADC-DAC interface card. The card had 16 inputs and 16 outputs, all of which had an operating range of -5 to $+5$ Vdc and 8-bit resolution. Conversion time for one channel of the ADC was 9 microseconds while the slew rate for the DAC was 10V/msec. Controlling subroutines were written in 6502 Assembler language while main programs were written in Applesoft Basic. A special purpose machine language display routine was developed which could update a screen display as often as 40 times a second.

The interface card performed 3 functions. It turned the

ion gun on and off by changing the gun bias voltage. It directly generated the dc sweep voltage applied in conjunction with the rf drive to the ring electrode. Finally it read the detector output and stored this information with the dc sweep voltage. The dc sweep was derived directly from the -5--+5V output of one of the DAC channels and coupled resistively to the ring electrode. The capacitive link to the rf transformer, grounded on the other end, imposed a high frequency limit on the sweep rate. The gun bias was controlled by a transistor in series with a variable dc power supply. Base current was supplied from one of the DAC channels through a resistor. It was possible to control the magnitude of the bias voltage by slight variations in the base current but for the experiments described later the transistor was just used as a switch. It was necessary to build a further amplifier and level shifter to maximize the resolution of the ADC. This was accomplished with an inverting op amp with the positive input tied low and the detector coupled capacitively with a large capacitor. (See figure 16 for a block diagram of the ion trap operating system.)

TRAP EXPERIMENTAL DATA AND RESULTS

Several preliminary experiments were performed with a view to calibrating the various instruments used to measure

the operating parameters of the trap. As mentioned before, the base pressure readings of the gas analyzer tube were compared against the readings from a Penning-style ionization gauge and found to be in rough agreement over the operating range of the Penning gauge. A calculation of the buffer gas pressure through use of the approximate compression ratio given for the turbomolecular pump when used with a helium residual gas and the foreline pressure measured with a thermocouple gauge was compared with the gas analyzer reading to get a measure of the buffer gas pressure when it was high. A known ac voltage was applied to the end cap electrodes and varied in order to get an experimental figure for the effective gain of the detection and amplification circuit. To get some idea of the ions available for trapping, the total ion current and the fraction reaching the far end cap through the hole in the near end cap were measured with no drive voltages applied.

The trap was first operated at the lowest pressure attainable (around 5×10^{-8} Torr) and with a high ion current. The output of the detection circuit showed a definite energy exchange between the ions and the tank circuit at the resonant frequency as the dc sweep varied the ion oscillation frequency through the tank resonant frequency. The "peak" manifested beats on either side of the main central peak and a tendency for the main peak to be positive, indicating the tank circuit was taking energy from the ions rather than the

other way around. The storage times were fairly short and the amplitude of the signal was low compared to those of later experiments. See figure 17.

The pressure in the chamber was then raised by allowing a controlled helium leak through a needle valve while the pump continued to function. As the helium background pressure increased, the peak became much more stable. With quite small background pressures it assumed the characteristic smooth negative peak with a small amount of ripple and overshoot on the sides. Increases in pressure up to the order of 10^{-4} Torr resulted in corresponding increases in the peak height. After 10^{-5} Torr the peak began to broaden noticeably and above 10^{-4} Torr the broadening became pronounced, while the amplitude ceased to increase and even diminished slightly. See figure 18.

With the buffer gas pressure maintained at around 10^{-4} Torr the trap was emptied and the gun turned off. The gun was turned on and the peak was scanned at .5 second intervals to observe the rate at which it grew with time. The trap was then filled and the gun turned off; the trap was again scanned at .5 second intervals to observe the decay of the signal with time. It was observed that from the point at which the peak was first observable to the point at which its height was stabilized it moved to the left. This indicated a frequency shift due to space charge in the trap which was used to calculate the ion density by the Fischer method. See

figure 19.

The amplitude of the detection signal and the amplitude of the dip in this signal shown by the peak height were used with the empirical model to calculate another value for the number of ions in the trap. This value was compared with the estimate of ion density given by Dehmelt's space-charge limited density and that given by Fischer's frequency shift estimate. The slope of the fill rate plot, coupled with a "best guess" estimate of the number of ions in the full trap, gives an estimate of the capture efficiency of the trap for ions injected through a hole along the z-axis of the trap.

CALCULATIONS

(A note concerning units: Dehmelt's formulae are derived in Gaussian units while Fischer and the empirical method, use MKS units. The formulae are expressed as they appear in the original texts in order to facilitate reference to them.)

1. Experimental data

Peak height of 4.4V corresponds to $dV=4 \times 10^{-3}V$.

Peak shift due to space charge = 1V.

$$r_o^2 = 2z_o^2 = 4 \times 10^{-4} m^2$$

Rf drive: 275 kHz, $V=200V$.

Detection drive: 50 kHz, $60 \times 10^{-3}V$.

Peak broadening: Q of resonant circuit = 150; $C = 500pF$;

$U_1 = 2.9V$; $U_2 = 3.5V$.

2. Ion density (Fischer method)

$$N = \rho/e = dU \times 4\epsilon_0 / r_o^2 e$$

$$= 6 \times 10^{11} / \text{m}^3$$

$$= 6 \times 10^5 / \text{cm}^3$$

3. Ion density (Dehmelt method)

$$N = 3V^2 / 16\pi m z_o^4 \omega_{rf}^2$$

$$= 2.6 \times 10^6 / \text{cm}^3$$

4. Actual number of ions

$$q = 2eV / m z_o^2 \omega_{rf}^2$$

$$= .5$$

$$a_1 = -4eU / m z_o^2 \omega_{rf}^2$$

$$= .015$$

$$a_2 = .018$$

$$\beta = (a - (a-1)q^2 / (2(a-1)^2 - q^2) - (5a+7)q^4 / (32(a-1)^3(a-4)) - (9a^2 + 58a + 29)q^6 / (64(a-1)^5(a-4)(a-9)))_{13}$$

$$\beta_1 = .384$$

$$\beta_2 = .389$$

$$Q_{ion} = \beta / d\beta = 80 \text{ (approx)}$$

$$N = d(V^2) / V^2 \times (C \omega_{ion}^2 m z_o^2 / 4e^2 Q_{res} Q_{ion})$$

$$= 8 \times 10^4 \text{ ions}$$

5. Trapping efficiency

In the first second of injection the peak reached approximately $1/4$ of its maximum; therefore 2×10^4 ions were trapped. The ion gun produced a current of about 1×10^{-8} amperes of which about 2×10^{-10} amperes entered the trap; this corresponds to about 10^9 ions/second. The capture efficiency is on the order of 10^{-5} .

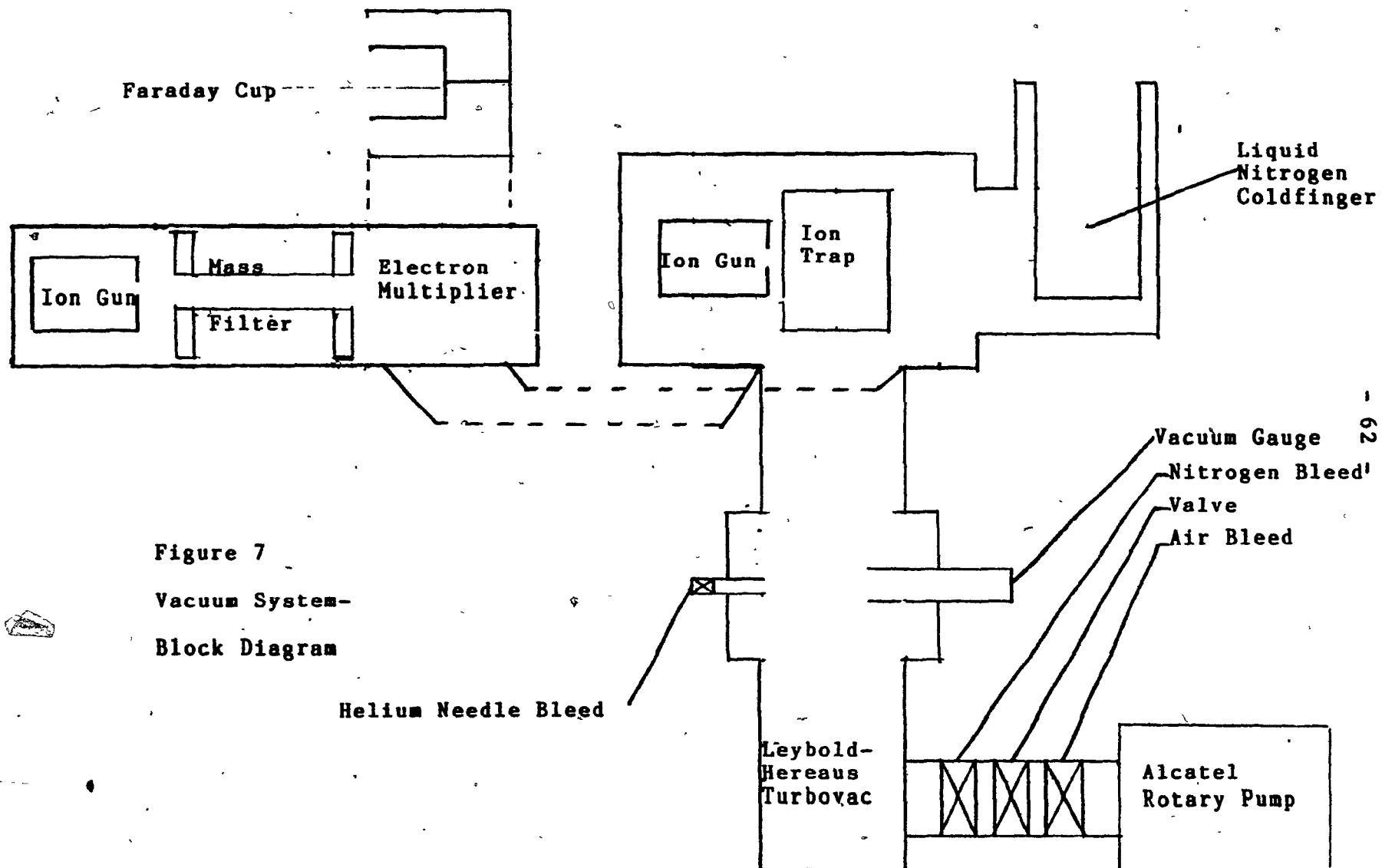


Figure 7
Vacuum System-
Block Diagram

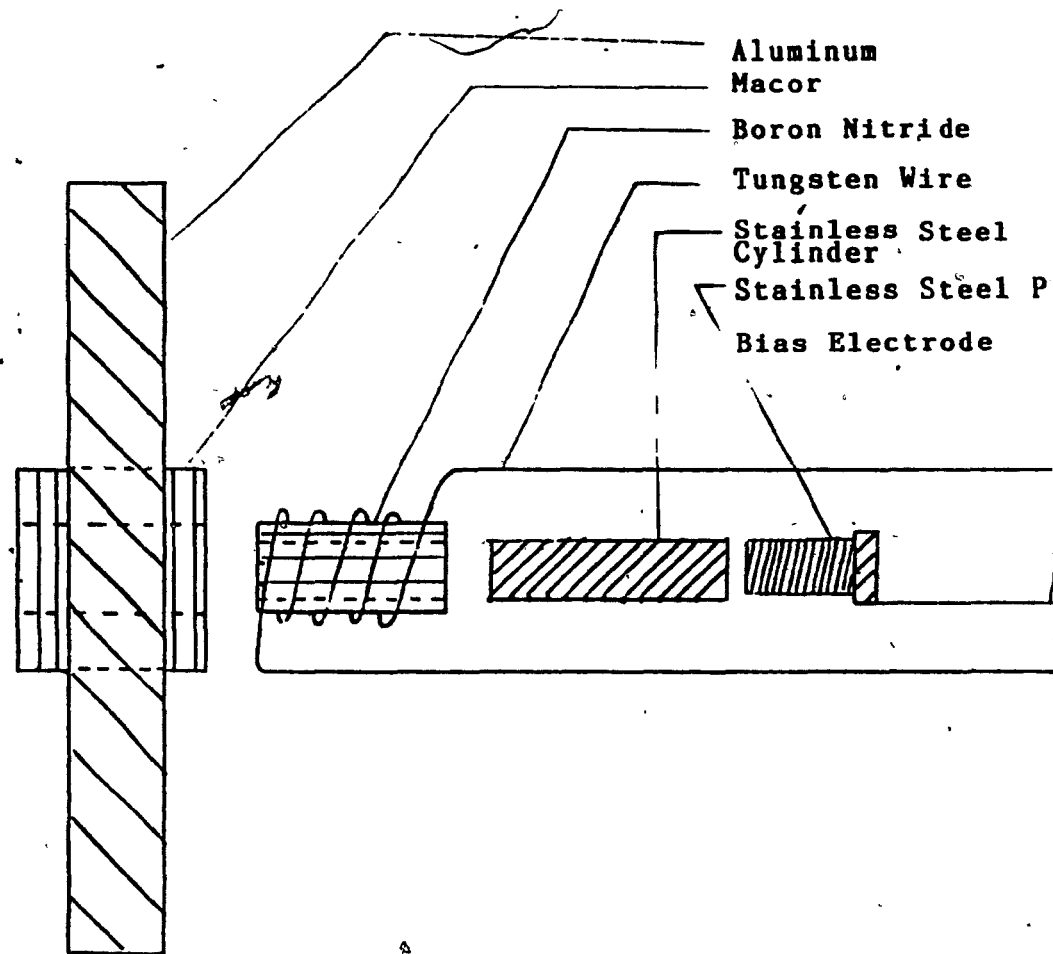
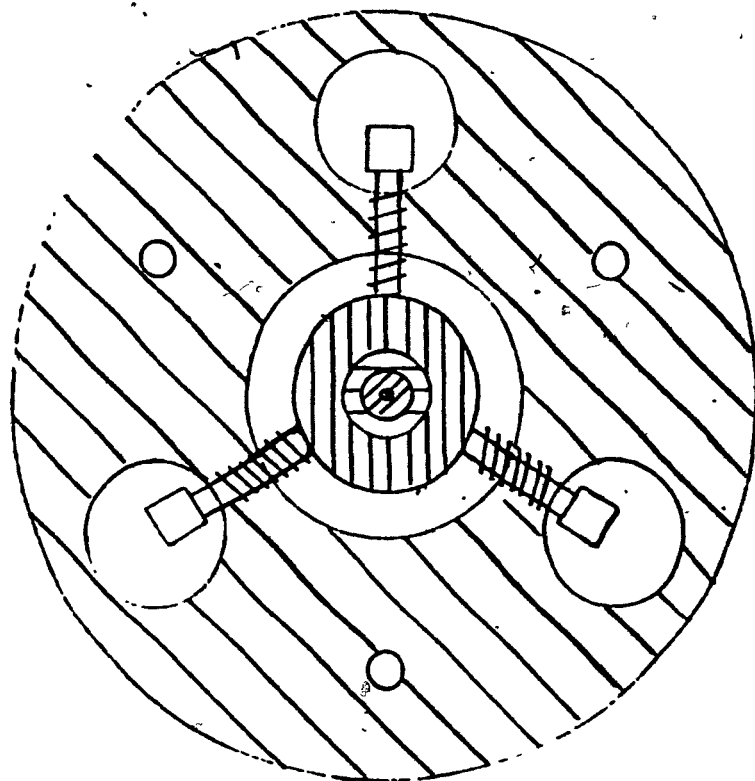


Figure 8 (not to scale)

Ion Gun with Mounting (sketch)

D. Young

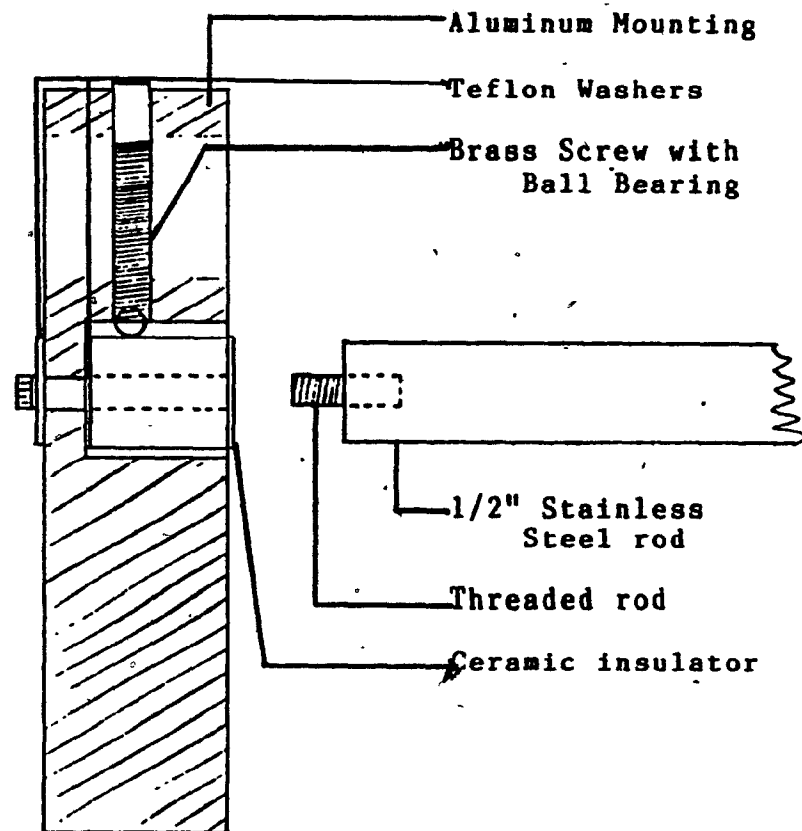
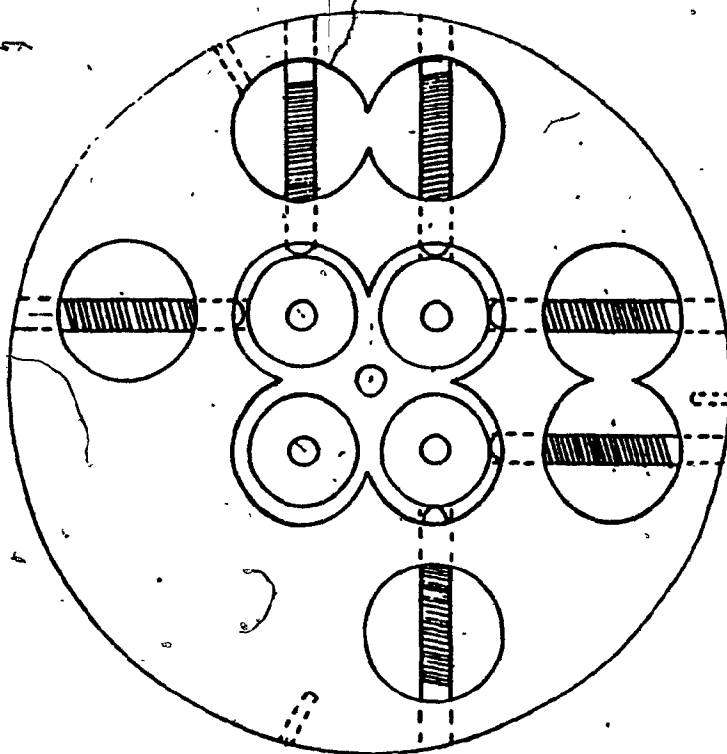
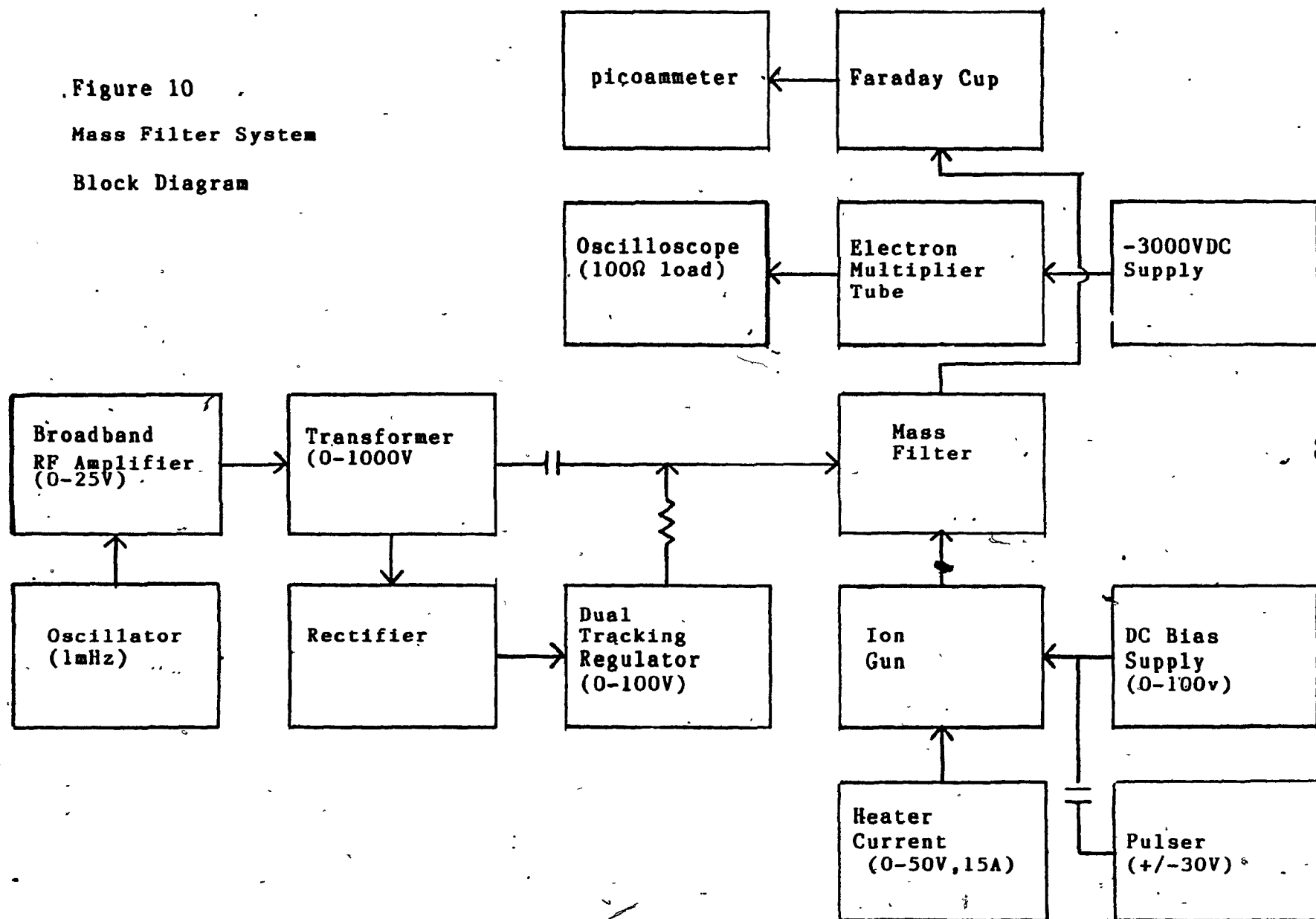


Figure 9 (not to scale)
 Mass Filter Details (sketch)
 D. Young

Figure 10
Mass Filter System
Block Diagram



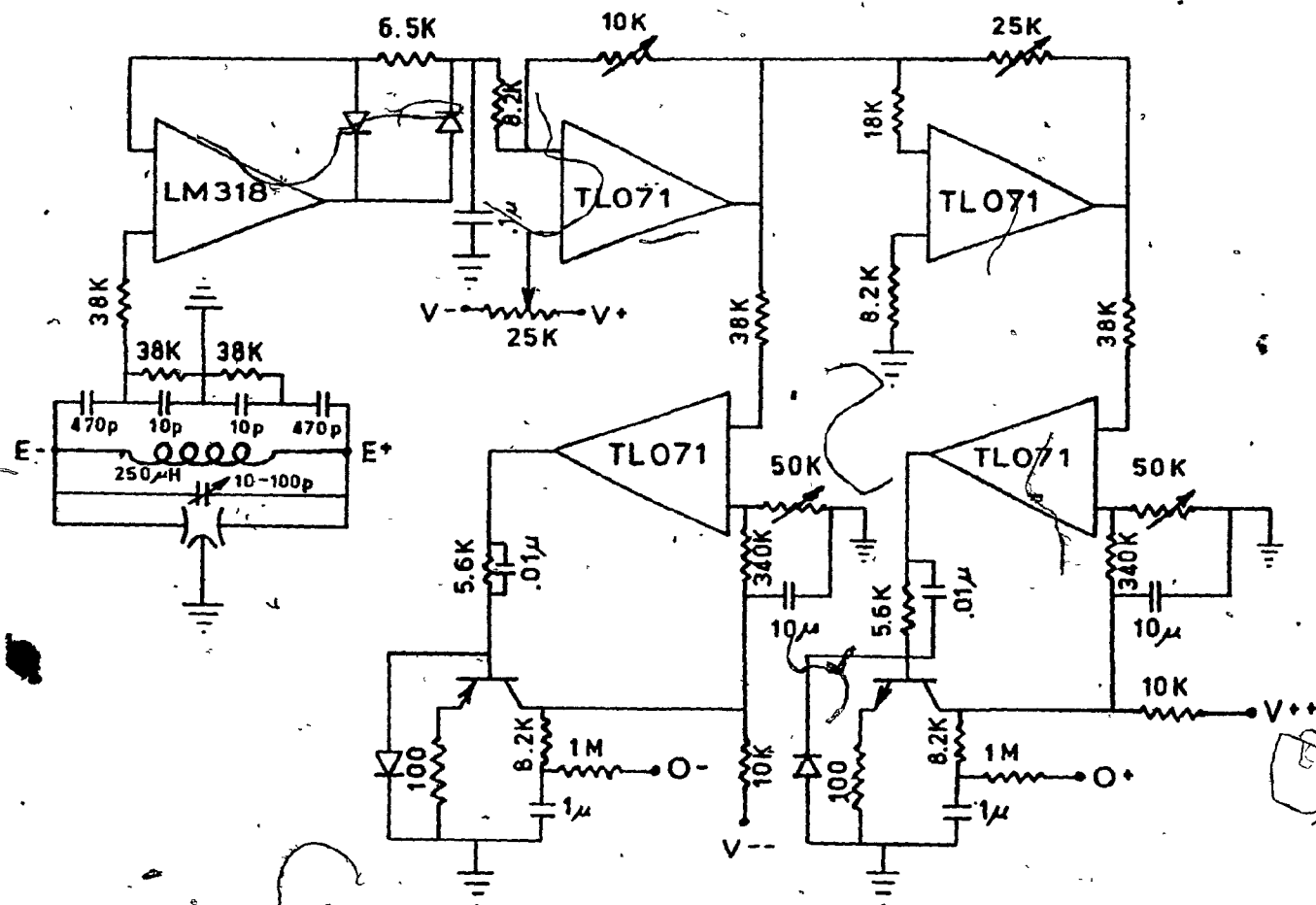
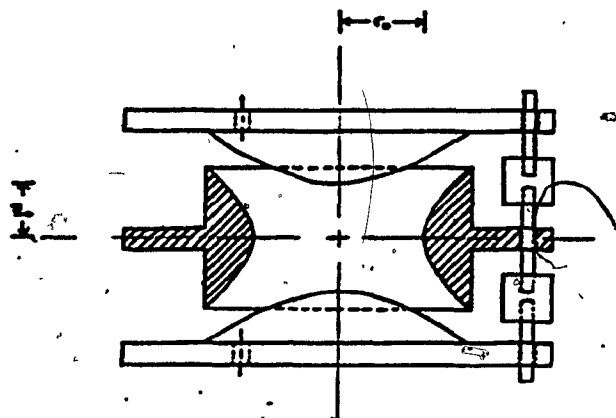


Figure 11
Mass Filter Rectifier and DC Supply
E+ and E- are connected to rod pairs

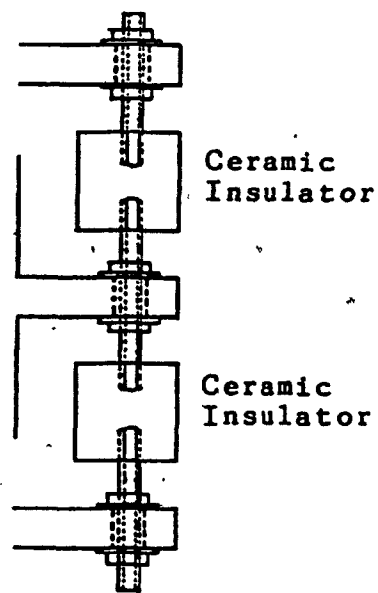
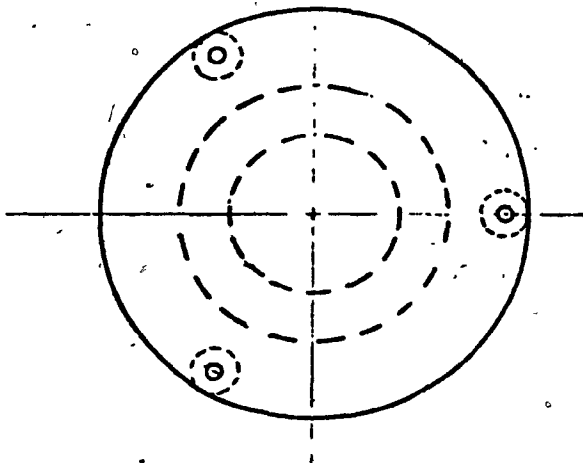
Figure 12

Ion Trap Details

D. Lunney



$$r_0 = 2\text{cm}$$
$$z_0 = 1.41\text{cm}$$

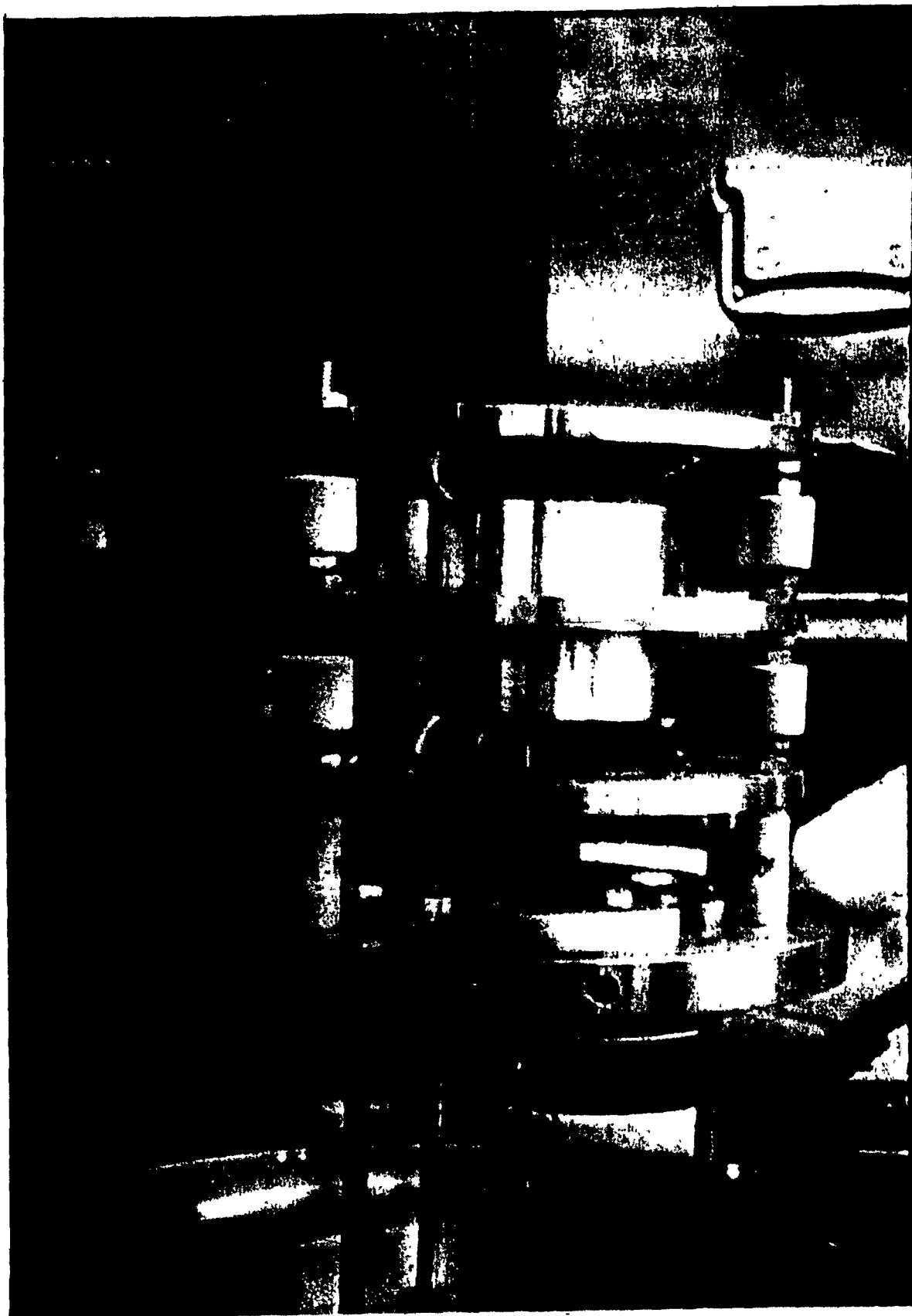


(This page deliberately left blank)

Figure 13

Photograph of the Ion Trap--Ion Gun Assembly

Photo by R. Moore

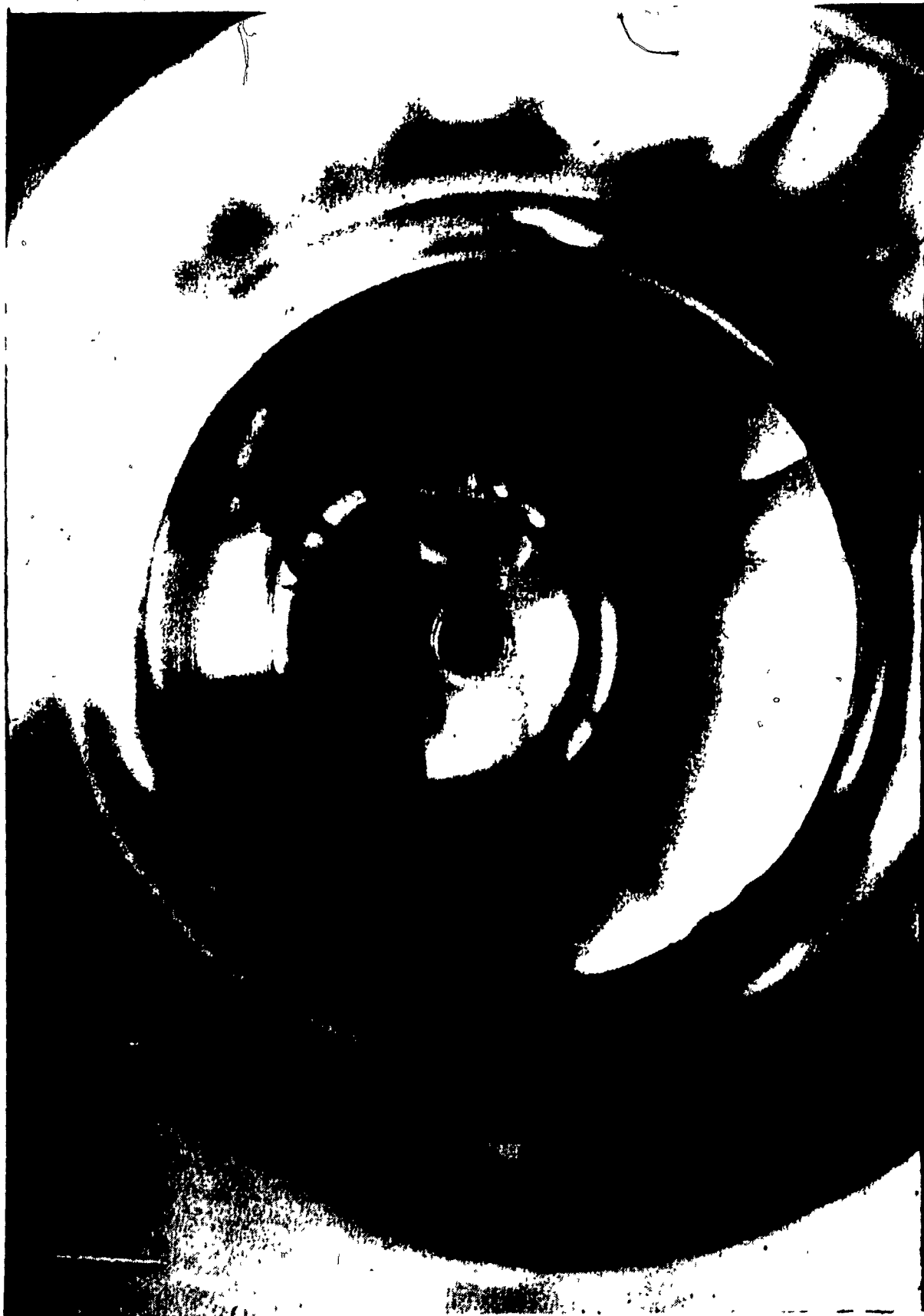


(This page deliberately left blank)

Figure 14

Trap Detail Showing Hole in End Cap

Photo by R. Moore



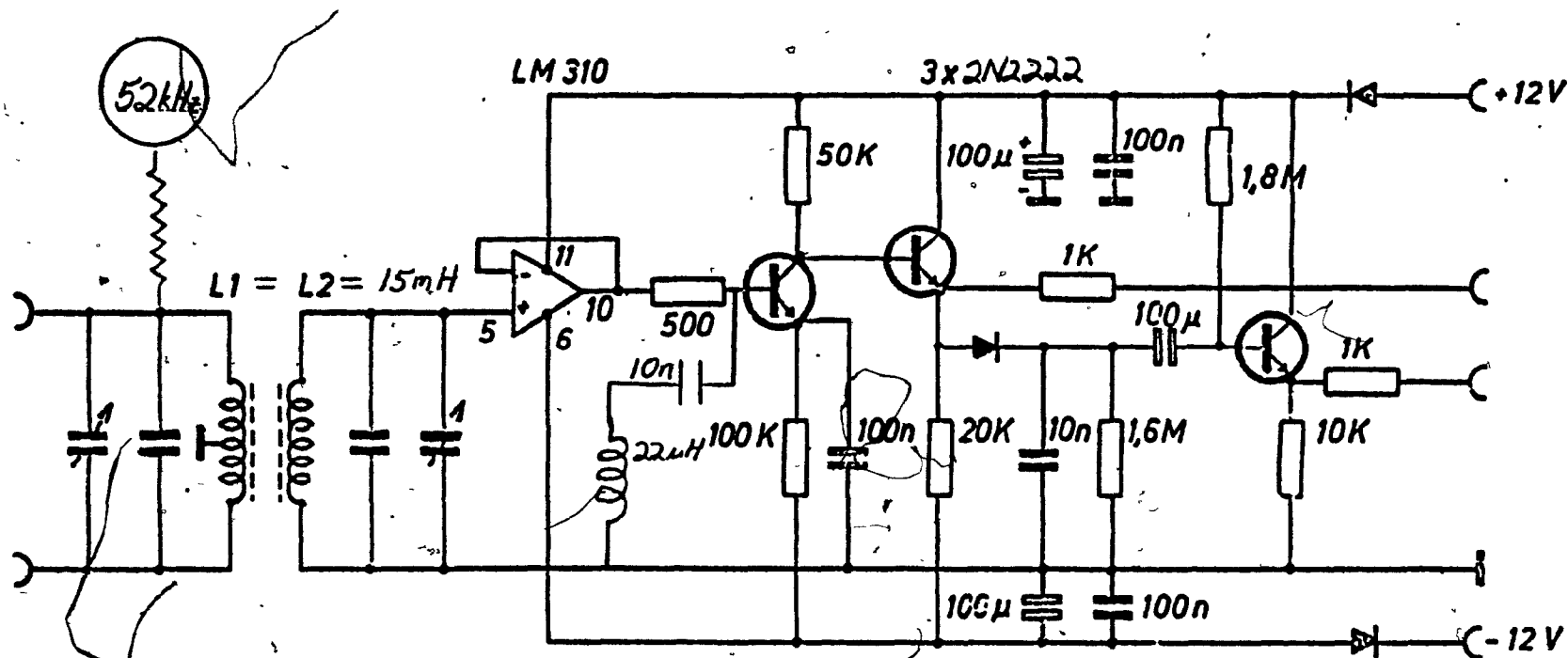
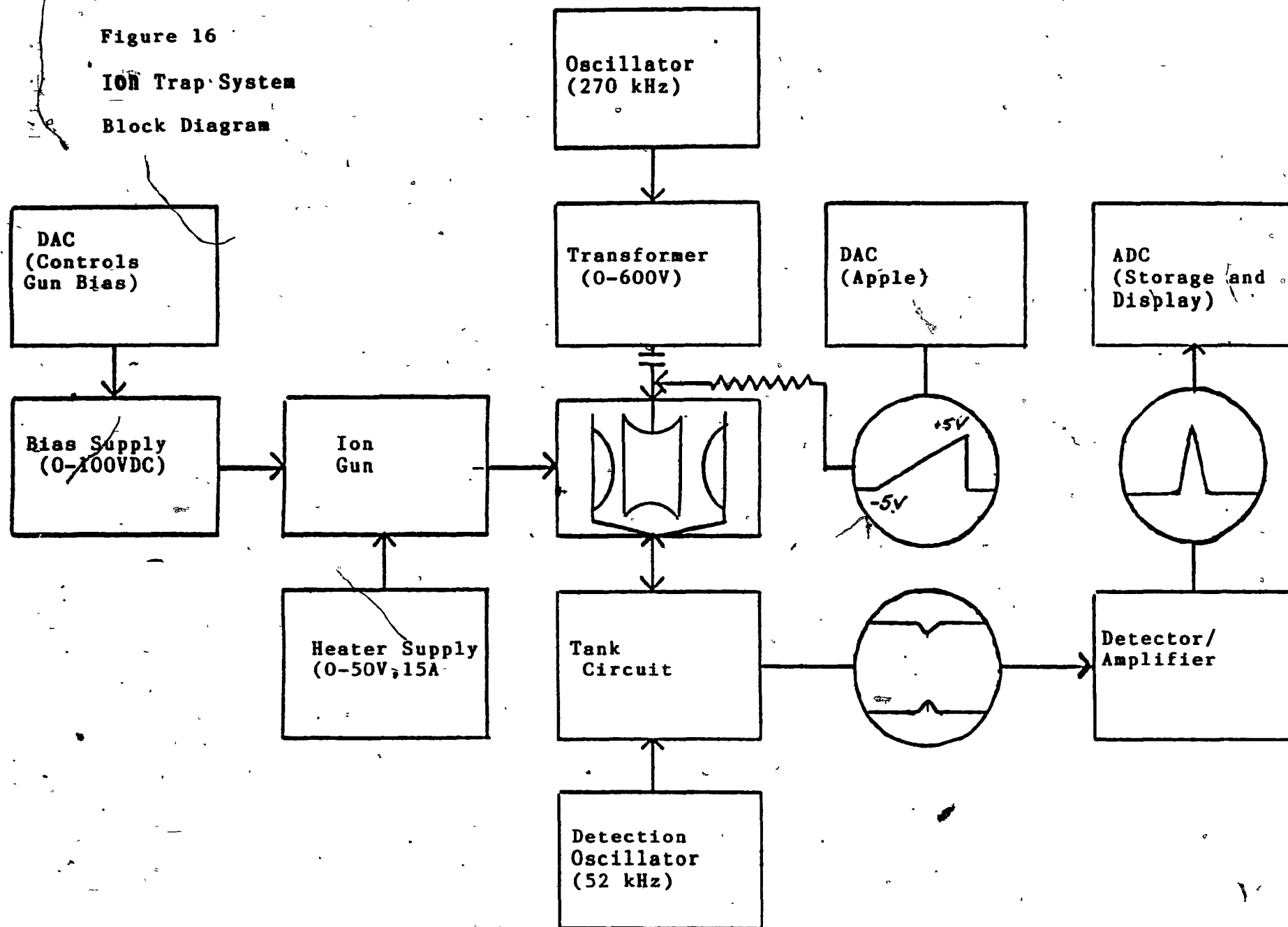


Figure 15

Ion Trap Demodulator-Amplifier Circuit

From Ifflander, Diplomarbeit

Figure 16
ION Trap System
Block Diagram



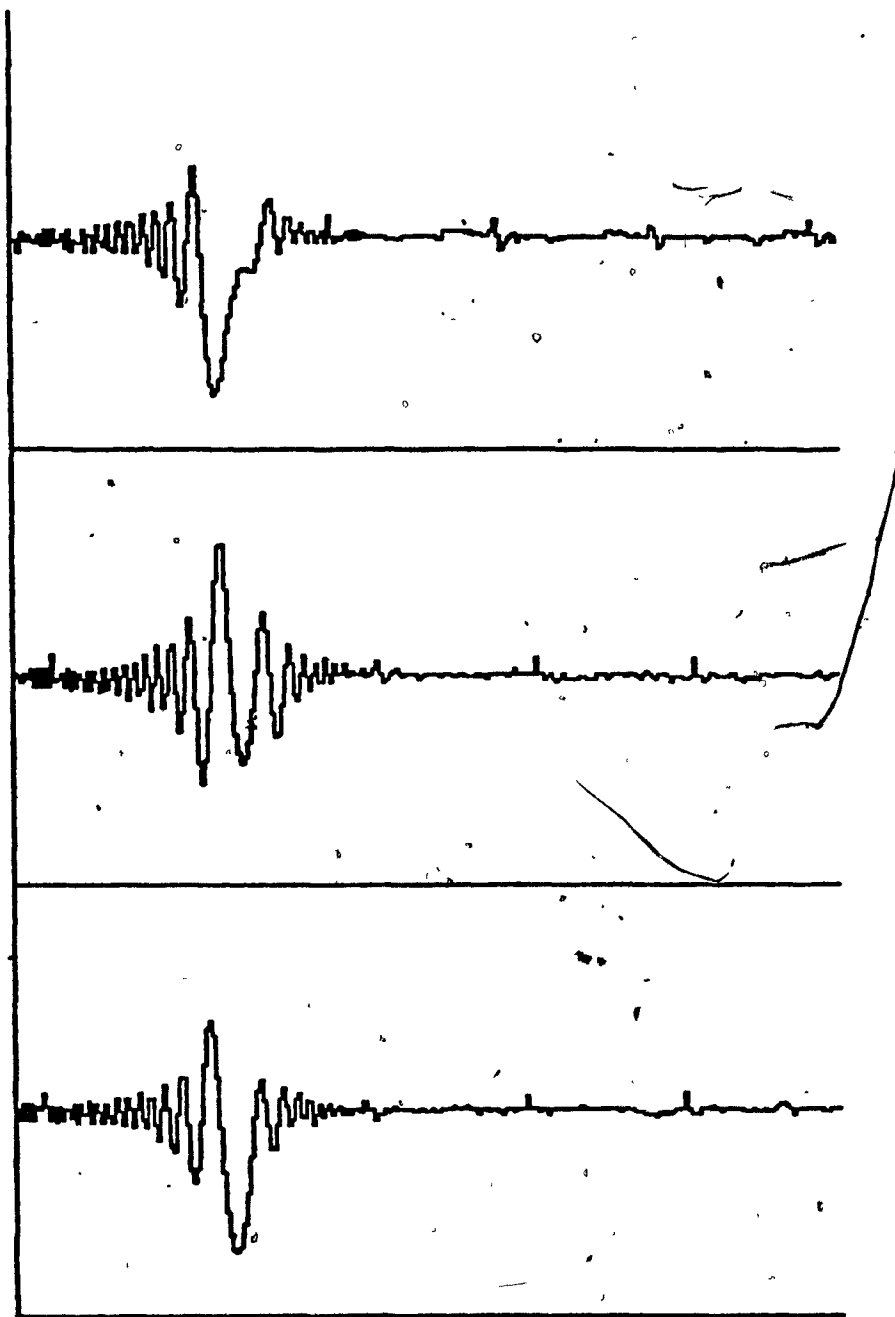


Figure 17

Representative traces with no buffer gas (10^{-7} Torr)

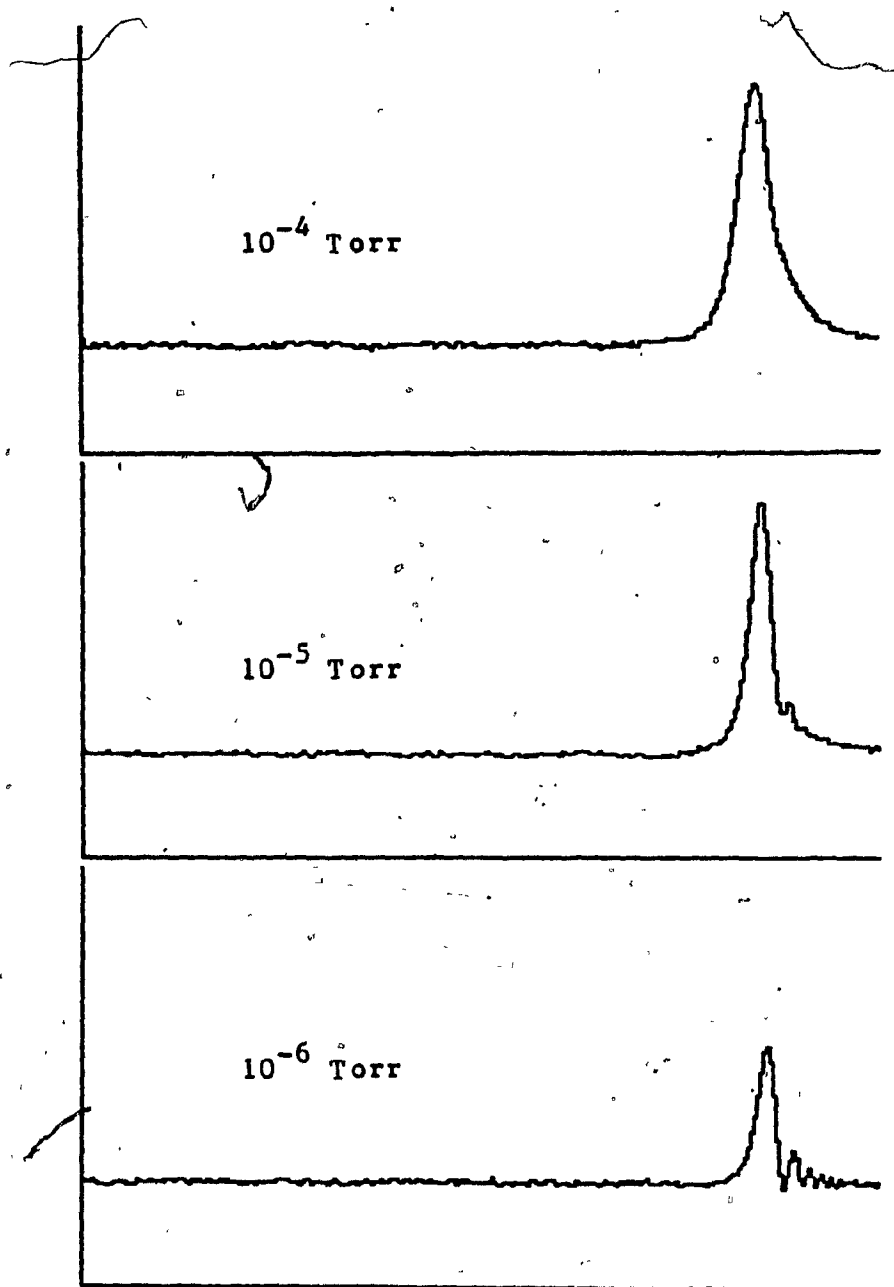


Figure 18

Traces showing effects of buffer gas on peak shape and amplitude

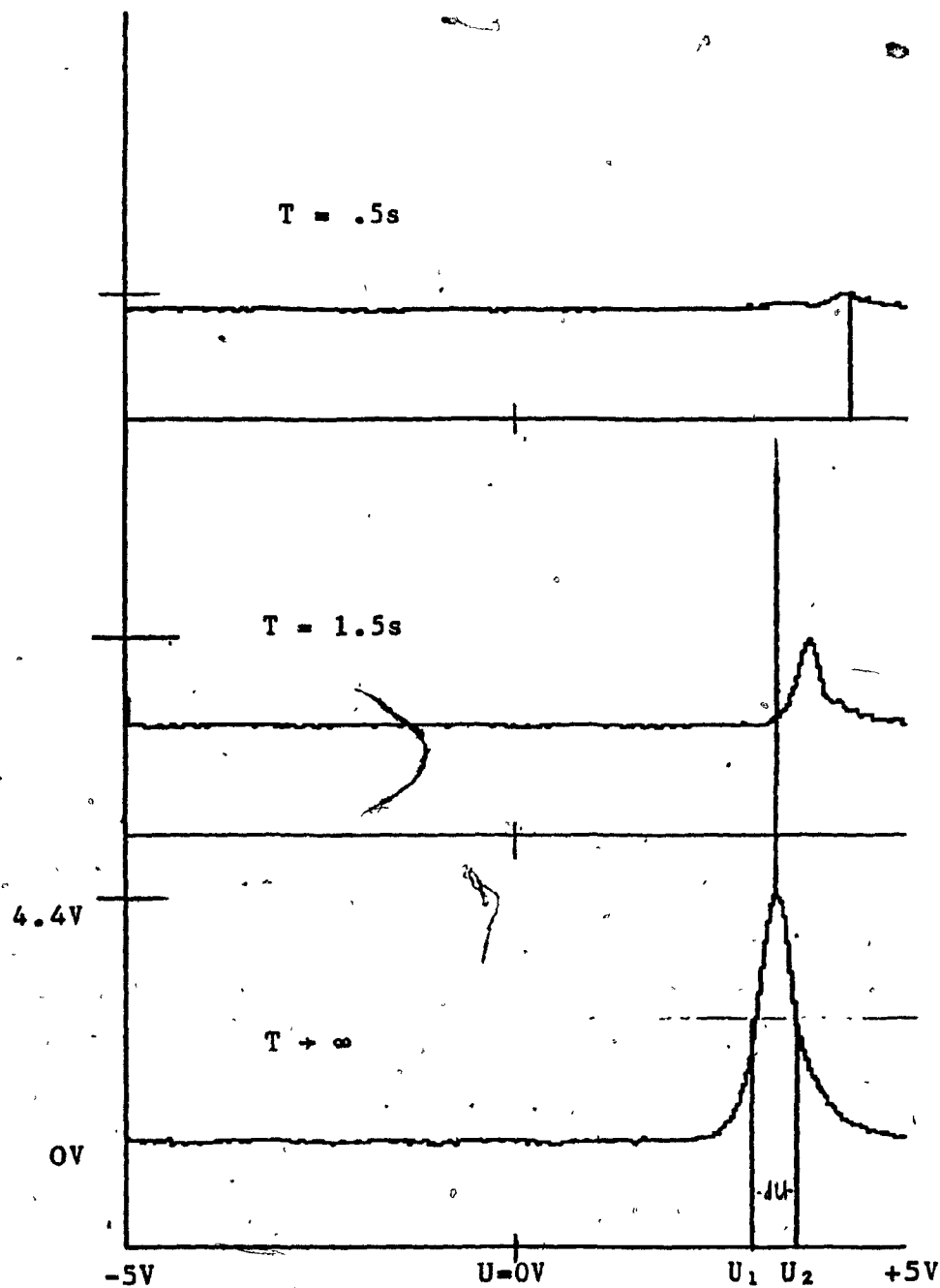


Figure 19

Successive traces showing frequency shift, fill rate and broadening (10^{-4} Torr)

REFERENCES--IV

1. Schinzler, B.; "Messung der Hyperfeinstruktur und Isotopieverschiebung in den Spaltungserzeugten Isotopen 138 139 140 141 142Cs Mit einer Kollinearen Anordnung Von Laser Und Teilchenstrahl", Doktorarbeit, University of Mainz, 1980
2. Weber; Cordes; "Aluminosilicate Ion Sources", Review of Scientific Instruments 37 (1966), pp. 118-119
3. Dawson (ref. 6, chapter 1); chapter 6 (written by Austin, W.; Holme, A.; and Leck, J.) describes the importance of proper alignment and offers some imaginative means to achieve it.
4. Langford-Smith, F. (ed.); Radiotron Designer's Handbook, Amalgamated Wireless Valve Co. - Ltd, Australia, 1953 (reproduced and distributed by RCA) Chapter 5 covers transformers.
5. Scroggie, M.; Wireless World 58 (1952), p. 89
6. The rectifier circuit was patterned after one found in Jung, W.; IC Op-Amp Cookbook, Howard Sams and Co., Indianapolis, 1979, chap. 5
7. The design of the dual tracking regulator followed principles and circuitry set forth in Horowitz, P.; Hill, W.; The Art of Electronics, Cambridge University Press, New York, 1980, chapter 5
8. Fischer; Z. Phys. 156 (1959), p. 26

9. Berkling, K.; Diplomarbeit, Bonn, 1956 (referenced by Dawson)
10. G. Rettinghaus; Zeitung Angew. Phys. 22 (1967), p. 321.
11. Schaaf; Schmeling; and Werth (see ref. 13, chapter 3)
12. The circuit was copied from a diagram found in Ifflander, R.; Diplomarbeit, University of Mainz. Similar circuits were employed by Paul and Fischer (see ref. 7, chapter 3)
13. Dawson (see ref. 6, chapter 1), p. 71

V CONCLUSIONS

It is easy to explain the apparent discrepancy between the number of ions calculated empirically and the ion densities predicted by Dehmelt and Fischer on the basis of the results of Knight and Prior noted above. If the ions are actually confined to a much smaller volume than the inscribed ellipse, then the densities of either the Fischer method or the Dehmelt method could be consistent with the smaller number of ions observed. It should also be noted that the trap was made of aluminum sitting in close proximity to a heat source. The base pressure in the trap was probably an order of magnitude higher than that indicated by the vacuum gauge and this would tend to make the trap less effective.

The trapping efficiency of 10^{-5} is nothing to be proud of but this is a first effort, with no effort to maximize the efficiency. The work of Schuessler and O suggests that certain angles of injection might be more likely to lead to capture than the one chosen; R. Moore has suggested that bunching the ions might make them easier to catch and that not only the rf drive frequency but also the much lower ion oscillation frequency might produce phase effects worth exploring. Lunney hopes in his thesis to mathematically explore some of these questions through consideration of a many-body model with the buffer-gas interaction taken into account.

At the Foster Radiation Laboratory a stainless steel trap with provisions for laser detection is under construction; our laser group is interested in the possibility of using the trap for high-precision measurement of nuclear properties of nuclei such as the various isotopes of strontium. Work on an on-line laser ion source is well under way and some interest has been expressed in the mass filter as a possible means for reducing background. While experimental work on radiofrequency mass spectrometric devices is a new development here, there is continuing interest in a wide range of applications of the preliminary research done on the properties of the rf quadrupole field.

BIBLIOGRAPHY

BOOKS

1. Arscott, F.M.; Periodic Differential Equations, MacMillan Co., New York, 1964
2. Becker, R.; Introduction to Theoretical Mechanics, McGraw-Hill, New York, 1954
3. Binns, K.; Lawrenson, P.; Analysis and Computation of Electric and Magnetic Field Problems, Pergamon, Toronto, 1973
4. Bronson, R.; Modern Introductory Differential Equations, McGraw-Hill, 1973
5. Dawson, P. (ed.); Quadrupole Mass Spectrometry and its applications, Elsevier Scientific Publishing company, New York, 1976.
7. Horowitz, P.; Hill, W.; The Art of Electronics, Cambridge University Press, New York, 1980
8. Jung, W.; IC Op-Amp Cookbook, Howard Sams and Co., Indianapolis, 1979
9. Kryloff, N.; Bogoliuboff, N.; Introduction to Non-Linear Mechanics, Princeton University Press, 1947
10. Langford-Smith, F. (ed.); Radiotron Designer's Handbook, Amalgamated Wireless Valve Co. Ltd, Australia, 1953 (reproduced and distributed by RCA).
11. Mathews and Walker; Mathematical Methods of Physics, Benjamin and co., New York, 1965
12. McLachlan, N.W.; Theory and Application of Mathieu Functions, Oxford at the Clarendon Press, 1947
13. Morse and Feshbach; Methods of Theoretical Physics, McGraw-Hill, New York, 1953
14. Steffen, K.; High Energy Beam Optics, Interscience publishers, 1964

ARTICLES

1. Berkling, K.; Diplomarbeit, Bonn, 1956

2. Courant; Livingston; Snyder; Physical Review 88 (1952), p. 1190
3. Dawson, P.; "A Detailed Study of the Quadrupole Mass Filter", International Journal of Mass Spectrometry and Ion Physics 14 (1974), pp. 317-337
4. Dawson, P.; Whetten, N, Naturwissenschaften 56 (1969), p.109
5. Dehmelt, H; "Radio Frequency Spectroscopy of Stored Ions I: Storage", Advances in Atomic and Molecular Physics 3 (1967)
6. Fischer; Z. Phys. 156 (1959), p. 26
7. Ifflander, R.; Diplomarbeit, University of Mainz
8. Knight, R.; Prior, M.; "Laser scanning measurement of the density distribution of confined $^6\text{Li}^+$ ions", Journal of Applied Physics 50(5) (1979), pp. 3044-3049
9. Maeda; Fukada; Sakimura; Mass Spectroscopy in Tokyo 17 (1969), 530
10. Major, F.; Dehmelt, H.; Physical Review 170 (1968), p. 91
11. Paul, W.; Steinweidel, H.; Z. Naturforsch A., 8 (1953) p.448
12. Rettinghaus; Zeitung Angew. Phys. 22 (1967), p. 321
13. Shaaf, H.; Schmeling, U.; Werth, G.; "Trapped Ion Density Distribution in the Presence of He-Buffer Gas", Applied Physics 25 (1981), pp. 249-251
14. Schinzler, B.; "Messung der Hyperfeinstruktur und Isotopieverschiebung in den Spaltungserzeugten Isotopen 138 139 140 141 ^{142}Cs Mit einer Kollinearen Anordnung Von Laser Und Teilchenstrahl", Doktorarbeit, University of Mainz, 1980
15. Scroggie, M.; Wireless World 58 (1952), p. 89
16. Schuessler, H.; Fortson, E.; Dehmelt, H.; "Hyperfine Structure of the Ion-Storage Exchange-Collision Technique", Physical Review V.187, #1, 5 November 1969
17. Schuessler, H.; O, C.; "Trapping of Ions Injected From An External Source Into A Three-Dimensional Quadrupole Trap", Nuclear Instruments and Methods 186 (1981), 219-30

18. Tamir, T.; Mathematical Computations 16 (1962), 77
19. Weber; Cordes; "Aluminosilicate Ion Sources", Review of Scientific Instruments 37 (1966), pp. 118-119
20. Wuerker, R.; Goldenberg, H.; Langmuir, R.; Journal of Applied Physics 30 (1959), 441
21. Wuerker, R.; Shelton; Langmuir, R.; Journal of Applied Physics 30 (1959), p.342